ARTHROPOD SYSTEMATICS & PHYLOGENY

76 (1): 147–172
14.5.2018

SENCKENBERG

Revealing species diversity of *Tomocerus ocreatus* complex (Collembola: Tomoceridae): integrative species delimitation and evaluation of taxonomic characters

Daoyuan Yu[1,2], Chunyan Qin[3], Yinhuan Ding[3], Feng Hu[1,2], Feng Zhang*[,3] & Manqiang Liu*[,1,2]

[1] Soil Ecology Lab, College of Resources and Environmental Sciences, Nanjing Agricultural University, Nanjing 210095, P. R. China; Daoyuan Yu [dyyu1987@hotmail.com, yudy@njau.edu.cn]; Manqiang Liu [liumq@njau.edu.cn]; Feng Hu [fenghu@njau.edu.cn] — [2] Jiangsu Collaborative Innovation Center for Solid Organic Waste Resource Utilization, Nanjing 210014, P. R. China — [3] Department of Entomology, College of Plant Protection, Nanjing Agricultural University, Nanjing 210095, P. R. China; Chunyan Qin [qinchunyan26@126.com]; Yinhuan Ding [2014102095@njau.edu.cn]; Feng Zhang [xtmtd.zf@gmail.com] — * Corresponding authors

Accepted 14.ii.2018.
Published online at www.senckenberg.de/arthropod-systematics on 30.iv.2018.
Editors in charge: Garvin Svenson & Klaus-Dieter Klass

Abstract. *Tomocerus ocreatus* species complex is among the commonest groups of Tomoceridae in East Asia and mainly distributed in the southern areas of China. Previous multi-locus molecular analyses have proved its monophyly and revealed extensive cryptic diversity within the complex. However, members of the complex are highly similar in traditional characters, thus morphological diagnosis have not been sufficiently developed in line with the molecular species delimitation. To update the taxonomy of the *ocreatus* complex, we carried out a molecular-morphological integrative study based on a wide-range survey of the complex in China. In addition to previous molecular analyses, we applied both distance and evolutionary model based methods on an enriched dataset of mitochondrial cytochrome c oxidase subunit I (COI) sequences. The molecular delimitation detected 20–36 molecular operational taxonomic units (MOTUs). In comparison, preliminary diagnosis based on traditional taxonomic characters distinguished only four morphological forms, while the characters previously thought to represent intraspecific variation distinguished 13 forms. According to a set of species validation criteria, the identities of nine independent species were acknowledged. Five new species: *Tomocerus huangi* sp.n., *Tomocerus pseudocreatus* sp.n., *Tomocerus virgatus* sp.n., *Tomocerus yueluensis* sp.n., and *Tomocerus zhuque* sp.n. are described, while *Tomocerus changbaishanensis*, *Tomocerus spinulus* and *Tomocerus zayuensis* are redescribed on the basis of holotype and/or topotypes. A key to the species of *ocreatus*-type tomocerids is provided. Incongruence across delimitation methods may be caused by incomplete sampling of populations and limitations of each method. The dorsal chaetotaxy, the prominent manubrial chaetae and the detailed morphology of dental spines were reviewed and confirmed to be valuable in the taxonomy of *Tomocerus*. The extensive diversity of the *ocreatus* complex in the southern areas of China indicates that tomocerid Collembola have much higher species richness than expected in the oriental realm. This study narrows species boundaries within the *ocreatus* complex and provides an example of how molecular approaches and detailed morphological examination can jointly benefit the exploration of biodiversity and the taxonomy of morphologically conservative groups of Collembola.

Key words. DNA barcoding, Automatic Barcode Gap Discovery, Poisson Tree Processes model, morphological characters, species delimitation, integrative taxonomy, key to species.

1. Introduction

Springtails (Collembola) are small wingless arthropods widely distributed and abundant in various terrestrial habitats. They feed on a wide range of food sources, such as microalgae, fungi, slime mould and detritus (Hopkin 1997; Hoskins et al. 2015; Potapov et al. 2016), and are among the main food sources to various invertebrate and vertebrate predators (Kopecky et al. 2016; Niffeler & Birkhofer 2017; Yin et al. 2017). Hence Collembola are of indispensable significance in the ecosystem function, especially in decomposition processes. Increasing attention has

been paid to Collembola in the research fields of systematics, ecology and agriculture (Deharveng 2004; Salmon et al. 2014; Forey et al. 2015; Reibe et al. 2015; Potapov et al. 2016; Widenfalk et al. 2016; Zhu et al. 2016). For most studies, precise identification of specimens to a desired taxonomic level is essential. However, the taxonomy of Collembola has not been sufficiently developed to meet this need in most areas of the world. In some groups, such as Tomoceridae Schäffer, 1896, the taxonomic system is still under construction and so far confusing.

Among Collembola, Tomoceridae are easily recognized by the relatively large body size (usually larger than 3 mm), the metal coloured scale coating, the usually long antennae, the elongated third abdominal segment and the well developed furca (jumping organ). Compared to other Collembola, Tomoceridae are relatively conservative in morphology; thus, morphology-based taxonomy has relied mainly on a limited number of characters, such as the general type and the arrangement of dental spines (spine-like chaetae on the middle segment of furca) and the number of teeth on the claws and mucro (distal segment of furca). Many species, such as *Tomocerus minor* (Lubbock, 1862) and *Tomocerus ocreatus* Denis, 1948, were defined mostly by these characters. However, species delimitation based only on traditional diagnosis has been challenged when molecular approaches are applied. By integrating molecular and morphological evidence, Felderhoff et al. (2010) and Park et al. (2011) described several species of *Pogonognathellus* (Börner, 1908) with similar morphology, and Barjadze et al. (2016) demonstrated in some cave-dwelling species of *Plutomurus* Yosii, 1956 that the number of claw teeth, dental spines and mucronal teeth were too variable within species to be used for diagnosis. Several attempts on molecular species delimitation have also unveiled extensive cryptic diversity among Tomoceridae in North America (Felderhoff et al. 2010), Europe (Porco et al. 2012) and East Asia (Zhang et al. 2014), resulting in the discovery of several species complexes. However, compared to the rapid rising of molecular taxonomy, progress in morphological species definition is still behind; as a result, many new forms remain undefined in those recently revealed species complexes.

An example for the taxonomic confusion of Tomoceridae is the *T. ocreatus* species complex. *Tomocerus ocreatus* was originally described from the tropical forest in the Southern Annamitic Cordillera, with the compound dental spines and the spine formula as main diagnostic characters. This species appears to be the most widespread tomocerid in East Asia (Yu et al. 2016a), and especially in the southern areas of China (Ma 2004). Variations in several characters, such as the prominent manubrial chaetae (Yosii 1967) and the detailed morphology of dental spines (Chiba 1968; Lee 1975; Martynova 1977), were treated as intraspecific and of less value than those traditionally important characters in species diagnosis. Recent studies have suggested that the group of species which were previously identified as *T. ocreatus* is in fact a monophyletic multi-species complex sharing a similar pattern of dental spines, with evidence from both molecular analysis of Chinese specimens (Zhang et al. 2014) and morphological review of the neotype of nominal species (Yu et al. 2016a). According to previous records and our collections, species of the *ocreatus* complex are mostly distributed to the south of the Qinling-Dabie Cordilleras of China. Variations in the previously less studied characters, such as the colour pattern or fine structure of dental spines, often occur across different forms. To date, two recently described species, *Tomocerus qinae* Yu, 2016 and *Tomocerus qixiaensis* Yu, 2016, have been distinguished from the other members of the *ocreatus* complex, but more comprehensive integrative study of this group has not been addressed.

To further explore the species diversity of the *ocreatus* complex, and to clarify the apparent ambiguity of several taxonomic characters, we carried out a molecular-morphological study on the available material of the complex. Molecular analyses were based on the 658 bp fragments of mitochondrial cytochrome c oxidase subunit I (COI) gene, which is a universal DNA barcode for Metazoa and has been frequently applied to various groups of Collembola (Porco et al. 2010; Schneider & D'Haese 2013; Katz et al. 2015; Sun et al. 2017). We also tested whether and how the variation of those traditionally important or less important characters can be of use in specific diagnoses, and to what extent the morphological identification matches the molecular delimitations.

2. Material and methods

2.1. Taxon sampling

Material for this study was collected mainly from the southern and eastern areas of China (Table S1). Samples were taken with aspirators and Berlese funnels and preserved in 99% ethanol before DNA extraction or morphological examination. Specimens were assigned to the *ocreatus* complex according to the habitus and the general type of dental spines after Zhang et al. (2014); the animals usually have white to yellow body colour, with varying coverage of bluish-purple pigment; the antennae are usually moderate to long in length; the dental spines are of compound type, with numerous secondary denticles on the surface. Four known species, *Tomocerus changbaishanensis* Wang, 1999, *T. qinae*, *Tomocerus spinulus* Chen & Christiansen, 1998 and *Tomocerus zayuensis* Huang & Yin, 1981, were included because they conformed to the criteria of the *ocreatus* group and were similar to some unidentified forms. All material studied is deposited in Nanjing Agricultural University (NJAU).

2.2. Molecular data acquirement

Forty-nine sequences of COI fragments with reliable specimen vouchers for morphological examination were extracted from reported works (Zhang et al. 2014; Yu et

al. 2016b), and the other 66 were newly introduced in the present study (Table S1).

DNA was extracted using an Ezup Column Animal Genomic DNA Purification Kit (Sangon Biotech, Shanghai, China) following the manufacturer's standard protocols. Extractions were performed non-destructively for further morphological examination and identification of the specimens. Primers were LCO1490/HCO2198 commonly used for Metazoa (Folmer et al. 1994). Amplification volume and procedure followed Zhang et al. (2014). All PCR products were checked on a 1% agarose gel. Successful products were purified and sequenced in both directions by Majorbio (Shanghai, China) on the ABI 3730XL DNA Analyser (Applied Biosystems). Sequences were assembled in Sequencher 4.5 (Gene Codes Corporation, Ann Arbor, USA), and deposited in GenBank (Table S1). Sequences were blasted in GenBank and checked for possible errors, then were preliminarily aligned using MAFFT v7.149 by the Q-INS-I strategy (Katoh & Standley 2013). Alignments were checked and corrected manually, with a final 658 bp alignment for COI.

2.3. Phylogenetic analyses

Neighbour-joining (NJ) trees and Kimura-2 parameter (K2P, Kimura 1980) divergences were calculated in MEGA 5.0 (Tamura et al. 2011). Node supports were evaluated through 1000 bootstrap replications.

Phylogenetic trees were reconstructed using maximum likelihood (ML) and Bayesian inference (BI) on online CIPRES services (Miller et al. 2010). *Tomocerus similis* Chen & Ma, 1997 was selected as the outgroup. To avoid the incorrect likelihood calculation, identical sequences were removed from the analyses. Best-fitting substitution models were assessed under the AIC and BIC criteria in jModelTest 2.1.7 (Darriba et al. 2012), with GTR+I+Γ model selected for subsequent analyses. ML trees were reconstructed in RAxML v8.2.4 (Stamatakis 2014) with GTRGAMMAI model and 1000 bootstrap replicates. BI analyses were conducted in MrBayes 3.2.6 (Ronquist et al. 2012). To avoid the problem of branch-length overestimation, the compound Dirichlet priors "br lenspr=unconstrained:uniform" for branch lengths were incorporated (Zhang et al. 2012). The number of generations for the total analysis was set to 50 million, with the chain sampled every 5000 generations. The burn-in value was 0.25 and other parameters were set as default. Evaluating effective sample size (ESS) values and state convergence were checked in Tracer 1.5 (Rambaut & Drummond 2007).

2.4. Molecular species delimitation

Both distance and evolutionary model based methods were employed. The Automatic Barcode Gap Discovery (ABGD) automatically clustered sequences into candidate species based on pairwise distances by detecting barcoding gaps (Puillandre et al. 2012). The ABGD analysis was carried out using a command-line version. Prior intraspecific divergence varied from 0.001 (Pmin, a single nucleotide difference) to 0.1 (Pmax), relative gap width was set to 1, with 20 recursive steps, 40 bids for graphic histogram of distances, K2P model for distance calculation and other parameters as default.

The Poisson Tree Processes model (PTP) tested species boundaries on non-ultrametric phylogenies by detecting significant difference in the number of substitutions between species and within species (Zhang et al. 2013). An unrooted ML tree was generated in RAxML v8.2.4 with the GTRGAMMA model and 1000 bootstrap replicates. Identical sequences were removed and Bayesian PTP (bPTP) delimitation was performed on single unrooted tree in python script bPTP.py v0.51 (Zhang et al. 2013). A total of 5×10^5 generations were run with first 20% as burn-in. Maximum likelihood delimitation (PTP ML) was also calculated in PTP.py v2.2 given 1000 trees derived from RAxML bootstrap analysis.

2.5. Morphological examination and description

Specimens were placed in morphological groups either according to traditionally important diagnostic characters or using characters previously thought to represent intraspecific variation within *T. ocreatus* (Table 1).

For morphological observation, specimens were cleared in Nesbitt's fluid and mounted in Marc André II solution. For some specimens, the head, furca and legs were dissected from the trunk and mounted separately for detailed observation. All separate legs were mounted in the same angle in lateral view for comparison. The slide-mounted specimens were studied using a Nikon Ni microscope. Specimens in alcohol were photographed using a Nikon SMZ1000 stereomicroscope with Nikon DS-Fi1 camera. Specimens on slides were photographed using a Nikon Ni microscope with Nikon DS-Fi1 camera.

For character description, we followed Fjellberg (2007) for interpretation of the maxilla, Yu et al. (2014) for the pattern of cephalic dorsal chaetotaxy and Christiansen (1964) for body macrochaetotaxy. The cephalic chaetotaxy is divided into 4 areas. The anterior and interocular areas are each subdivided into front row and hind row, the postocular and posterior areas are each subdivided into left and right sides; numbers of macrochaetae in different rows/sides are separated by a comma/plus sign. The description of the body chaetotaxy referred to one side only as most cases two sides are symmetrical. The exact morphology of each chaeta was unclear due to shedding. The dental spine formula follows that of Folsom (1913), in which the dental spines are arranged from basal to distal, with a slash indicating the separation between basal and medial subsegments and the bold font referring to spines that are noticeably larger. If not mentioned specifically, all descriptions were based on fully developed individuals.

Table 1. Status of morphological diagnostic characters and corresponding grouping of the *ocreatus* complex species in this study. — ***Abbreviations:*** AG = groups most supported by ABGD method; PG = groups most supported by PTP method; TG = groups delimitated by traditional characters; MG = groups delimitated by combination of potential and traditional characters; ma = dorsal macrochaetae on the anterior area of head; ug = number of ungual inner teeth; ds = type of dental spines; df = dental spines formula; mt = mucronal intermediate teeth; cm = number of central macrochaetae on Th. II; msc = status of manubrial scales; mp = number and shape of prominent chaetae on manubrium and basal part of dens; pp = position of prominent chaetae on manubrium if only 1+1 present; dd = size of denticles on dental spines (s = small; m = moderate; l = large). Question mark (?) = status not seen or with uncertainty; hyphen (–) = character not existing.

Traditional characters					TG	Potential characters					MG	AG	PG	Species/groups
ma	ug	ds	df	mt		cm	msc	mp	pp	dd				
2,4	5–6	compound	3–5/4–5, **1**	4–7	1	6	narrow band	1+1,1, pointed	middle	s–m	1	1	1	*T. spinulus*
2,4	5–6	compound	1–2, **3**–**4**/4–5, **2**	5–7	2	6	narrow band	1+1,1, blunt	distal	s	2	2	2+3	*T. zhuque* sp.n.
2,4	5–6	compound	4/3–4, **1**,1, **1**	6–7	3	6	narrow band	2+2,1, pointed	—	s	3	3	4	*T.* cf. *folsomi*
2,4	5–7	compound	5–6/4, **2**	5		6	broad band	2+2,1, pointed	—	s	4	4	5	*T. zayuensis*
2,4	5–6	compound	4/4–5, **2**	3–9		6	narrow band	not distinct	—	s	5	5	6	*T. huangi* sp.n.
2,4	5–7	compound	4–5/3–5, **2**	4–7		6	narrow band	1+1,0, blunt	distal	m–l	6	6	7	*T. changbaishanensis*
2,4	6	compound	3–4/2–3, **2**	5–6		5	absent	2+2,1, blunt	—	m	7	7	8	*T. pseudocreatus* sp.n.
2,4	5–6	compound	3–4/3–4, **2**	5–7		5	absent	1+1?,1, blunt	distal	m	8	8	9	undefined group
2,4	5–6	compound	3–4/4, **2**	5–6		5	absent	1+1?,1, blunt	distal	m		9	10	undefined group
2,4	6	compound	4–5/2–4, **2**	7–8		5	absent	2+2,1, pointed	—	m	9	10	11	*T. yueluensis* sp.n.
2,4	5–6	compound	4/3, **1**,0–1, **1**	5–7		5	absent	not distinct	—	m	10	11	12	undefined group
2,4	5–7	compound	4/3–4, **1**,0–1, **1**	6–7	4	5	absent?	not distinct	—	m		12	13+14+15	undefined group
2,4	5–6	compound	4/4, **2**	5–6		5	narrow band	2+2,1, pointed, weak	—	m	11	13	16	*T.* cf. *qinae*
2,4	6	compound	4/4, **2**	7–8		6	narrow band	not distinct	—	m		14	17	*T.* cf. *qinae*
2,4	5–6	compound	4/5, **2**	8–9		6	narrow band	not distinct	—	m		15	18	*T.* cf. *qinae*
2,4	4–6	compound	4–5/4–5, **2**	5–9		5–6	narrow band	not distinct	—	m		16	19	*T. qinae*
2,4	5	compound	4–5/3–4, **2**	6		1	absent	not distinct	—	m–l	12	17	20	*T. virgatus* sp.n.
2,4	5–6	compound	4/3, **2**	5–7		1	several	?	—	m–l	13	18	21	*T.* cf. *ocreatus*
2,4	5–6	compound	5/2–3, **2**	6–7		1(2?)	several	?	—	m–l		19	22	*T.* cf. *ocreatus*
2,4	5–6	compound	3–4/2–3, **2**	7–8		1?	narrow band	not distinct	—	l		20	23	*T.* cf. *ocreatus*

2.6. Species validation criteria

In the present study, the validation of species was performed on the basis of consensus across grouping strategies derived from a range of analyses (Carstens et al. 2013) by the following criteria: **(1)** monophyletic lineage confirmed by phylogenetic inferences, usually with reliable genetic distance between lineages; and **(2)** reliable and stable morphological difference across lineages and congruence within lineage. For incompatible grouping strategies across different analyses, re-examinations were performed carefully by the following procedure: **(1)** check if there were under- or overestimated morphological characters through detailed observation in more specimens; **(2)** check if the molecular grouping could be affected by incomplete sampling given the geographical and morphological information; and **(3)** question or abandon the results rejected by their own irrationality and/or by their incongruence with other analyses, when there is strongly supported correspondence among others.

2.7. Abbreviations

Morphology: **Abd.** – abdominal segment; **Ant.** – antennal segment; **PAO** – postantennal organ; **Th.** – thoracic segment. ***Species delimitation***: **AG** – groups most supported by ABGD method; **MG** – groups delimitated by combination of potential and traditional characters; **PG** – groups most supported by PTP method; **TG** – groups delimitated by traditional characters. ***Institution***: **NJAU** – Nanjing Agricultural University, Nanjing, China.

3. Results

3.1. Species delimitation

The ABGD method generated nine sets of valid partition strategy. According to detected prior intraspecific divergence (*P*) between 0.001 and 0.0599, 20 and 36, 31, 27, 25, 23, 20 MOTUs were recognized in initial partitions and recursive partitions, respectively. Initial and recursive partitions were congruent at $P = 0.0599$ while the number of MOTUs was 20 (Fig. 1A). Because the initial partitions were stable on a wider range of prior values and were usually close to the hypothetical species number described by taxonomists (Puillandre et al. 2012), the value 20 was preferred as the result of ABGD before intercalibration across all analyses. Among the 20 groups (AGs), the maximum K2P distance within group was 0.0540 in AG2; the minimum and maximum between group distances were 0.0763 between AG14 and AG15 and 0.2226 between AG16 and AG17 (Table S2). The approximate barcoding gap was 0.06–0.075 (Fig. 1B).

The bPTP delimitation range was estimated as 21–27 (mean 23.41) MOTUs based on the single unrooted tree; the PTP ML delimitation recognized 20–27 (mean 23.13) MOTUs based on multiple bootstrap trees. A number of

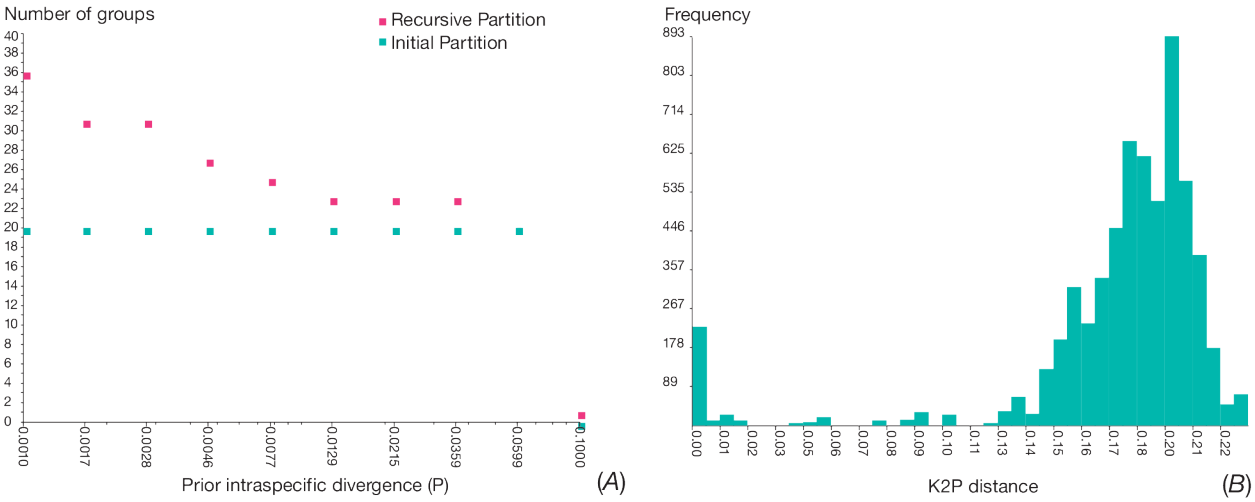

Fig. 1. ABGD species delimitation. **A**: Frequency histogram of K2P pairwise divergences. **B**: Partitions under different prior intraspecific divergences.

23 MOTUs (PGs) was best supported in both PTP analyses (Fig. 2).

Great disparity was shown between the results of molecular analyses and the morphological diagnosis based on only traditional characters, which recognized only 4 morphological forms (TGs) among the species complex. In comparison, 13 forms (MGs) were distinguished when both potential and traditional characters were involved (Table 1).

Integrating the results of all approaches, the grouping strategy by traditional diagnosis was abandoned because of its extremely low resolution and deep incongruence (4TGs versus 13MGs, 20AGs and 23PGs) with other analyses. The outputs of ABGD and two PTP approaches overlapped in the interval of 20–27 groups though the best supported results were 20 AGs and 23 PGs, with AG2 and AG12 subdivided into three and two PGs, respectively. Further integrative analysis showed that AG2 and AG12 were not to be subdivided as the best supported PTP results, for the following reasons: **(1)** both AG2 and AG12 formed strongly supported monophyletic lineages (Fig. 2); **(2)** strong morphological congruence was present within groups; **(3)** within each group, specimens were from the same or nearby localities; **(4)** the grouping corresponded well with the barcoding gap of 0.06–0.075; and **(5)** 20 MOTUs were also supported in PTP ML approach as a lower limit. The morphological diagnosis including potential characters performed better than traditional diagnosis, but still did not distinguish all MOTUs, with MG8 = AG(8+9), MG10 = AG(11+12), MG11 = AG(13+14+15+16), MG13 = AG(18+19+20), while the other MGs coincided with AGs. Further examination indicated that colour pattern was potential diagnostic characters for the AGs (Fig. S2). However, several AGs had within-group variations in colouration, especially between specimens of different sizes. Further, the stability of colouration varied in different AGs, thus the exact boundaries between some similar AGs was still unclear.

3.2. Taxonomy

According to our consensus criteria for species validation, nine independent species in the complex were determined at this stage. Because topotypes of *Tomocerus folsomi* Denis, 1929 from Yunnan Province was not retrieved for the study, the identity of morphologically similar species AG3 = MG3 = PG4 = TG3 from Guizhou Province was unclear and not described. Other species, including three known and five new to science, are described below in alphabetical order. A key to the known species of *T. ocreatus* complex is provided.

Subfamily Tomocerinae Schäffer

Genus *Tomocerus* Nicolet

Tomocerus Nicolet, 1842: 67.

Type species. *Macrotoma minor* Lubbock, 1862: 598

Diagnosis. Moderate to large Tomocerinae, usually longer than 3 mm; body colour pale to dark, some species with distinct colour pattern; eyes at most 6+6; labral formula typically 4/5, 5, 4, rarely 6/5, 5, 4; distal edge of labrum with 4 papillae ending in curved spines; mentum with 5 chaetae, submentum with numerous chaetae; mandibular head asymmetrical, the left side with 4 teeth and the right side with 5 teeth, left molar plate distally with a tapered tooth; maxillary lamella 5 without beard-like appendage; maxillary outer lobe with trifurcate palp, one basal chaeta and 4 sublobal hairs; Ant. I and Ant. II scaled, Ant. III unscaled or basally scaled, Ant. IV unscaled; macrochaetae densely arranged along anterior margin of Th. II (not shown in figure) and sparsely on each terga, most mesochaetae laterally and posteriorly on terga; trochanterofemoral organ reduced to 1 slender chaetae on each segment; each tibiotarsus with a distal whorl of 11 chaetae, ventral six as ordinary chaetae, dorsal five modified as a

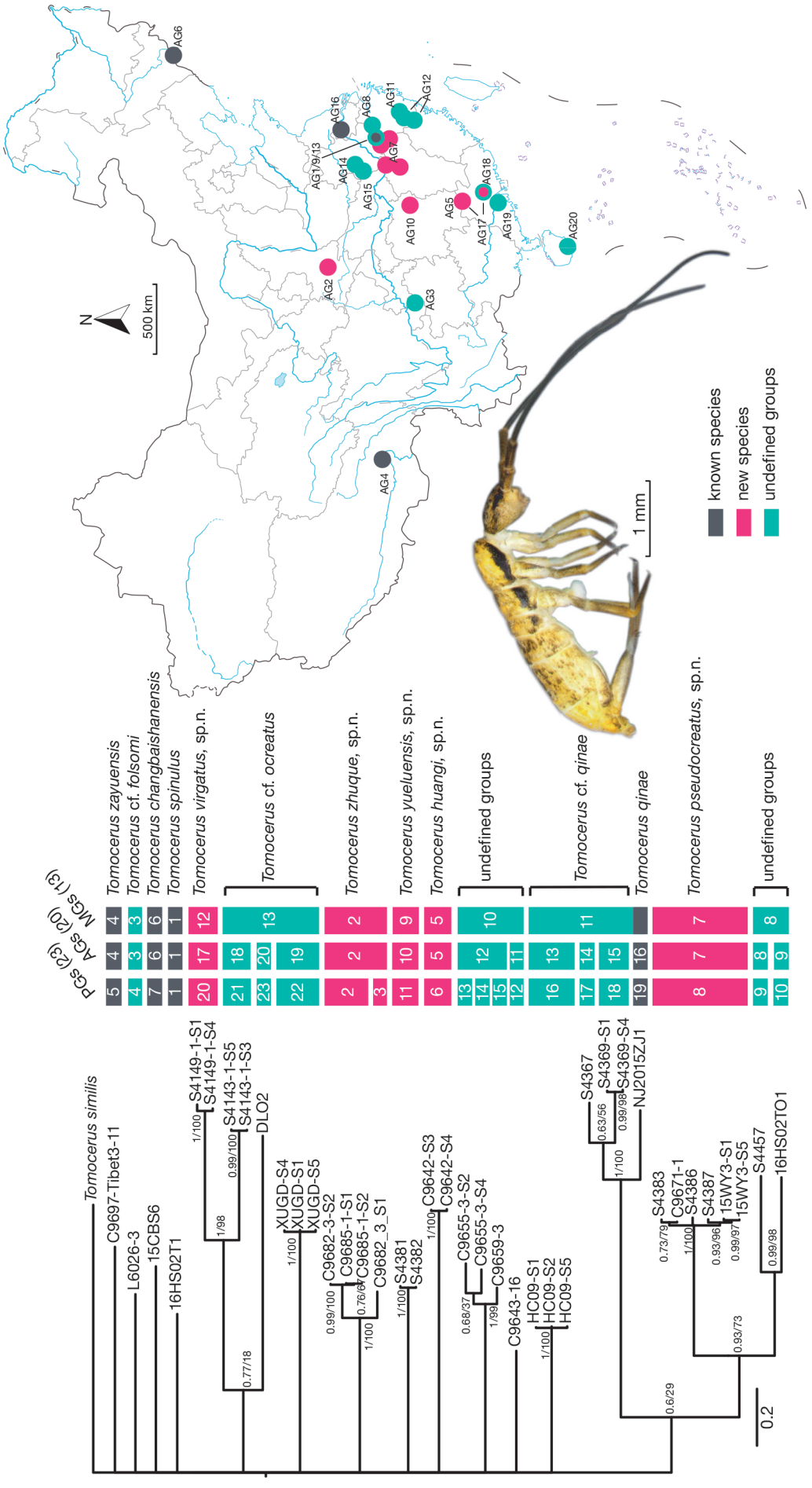

Fig. 2. Phylogenetic tree, sampling map and typical habitus of the *ocreatus* complex species. The tree summarizes the best supported grouping strategies by ABGD (AGs), PTP approaches (PGs) and morphological diagnosis (MGs). Grouping by traditional diagnosis (4 TGs) is not shown. The tree topology is from Bayesian phylogenetic reconstruction. The posterior probabilities/likelihood bootstraps are marked on nodes. The AGs are marked in the collecting localities on an outline map of China. Colored bars and dots represent species groupings based on corresponding delimitation analyses. Numerals in bars represent group numbers. Profile of specimen: *Tomocerus qinae* Yu, 2016.

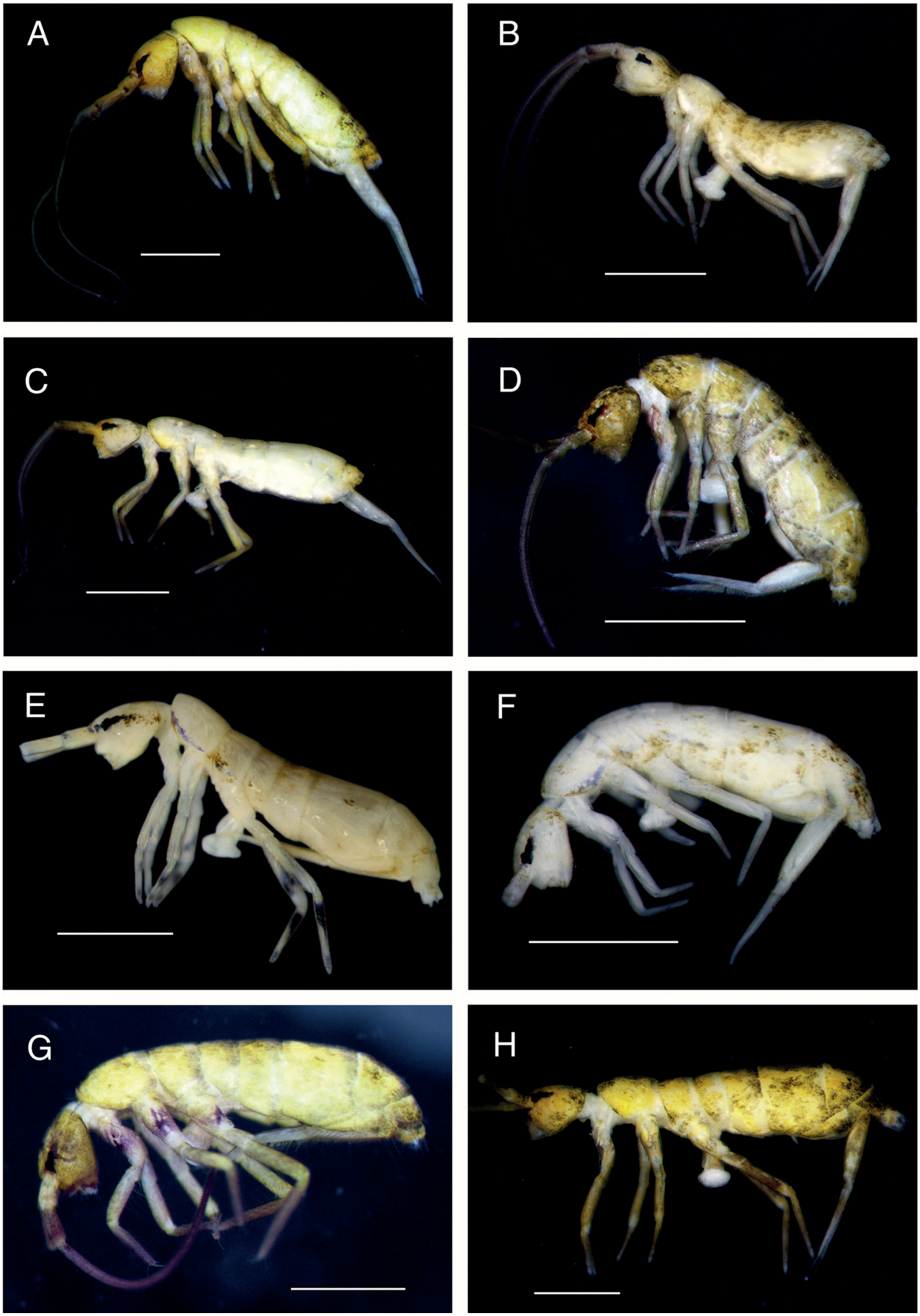

Fig. 3. Appearance of specimens in alcohol, lateral view, left side. **A**: *Tomocerus changbaishanensis* Wang, 1999. **B**: *Tomocerus huangi* sp.n. **C**: *Tomocerus pseudocreatus* sp.n. **D**: *Tomocerus spinulus* Chen & Christiansen, 1998. **E**: *Tomocerus virgatus* sp.n. **F**: *Tomocerus yueluensis* sp.n. **G**: *Tomocerus zayuensis* Huang & Yin, 1981. **H**: *Tomocerus zhuque* sp.n. (Scale bars: 1 mm)

central tenent hair, a pair of accessory chaetae and a pair of guard chaetae; rami of tenaculum with 4+4 teeth; dens of furca basally without outer strong chaetae or inner large differentiated scales; shape of dental spines from simple to compound among different species; mucro elongated, bearing numerous smooth chaetae with elongated sockets (not shown in figure); two mucronal dorsal lamellae running from subapical tooth, outer lamella ending in inner basal tooth, inner lamella ending at base of mucro, intermediate teeth located on outer lamella; both mucronal basal teeth with proximal lamellae, outer basal tooth usually with corner toothlet.

Tomocerus ocreatus complex (Zhang et al., 2014)

Diagnosis. Body size normal for *Tomocerus*; body colour usually white to yellow with varying coverage of bluish-purple pigment, seldom grey or dark; antennae usually subequal to or longer than body, seldom short; bothriotricha 2, 1/ 0, 0, 1, 2, 0, 0 on Th. II–Abd. VI; dental spines compound, with numerous secondary denticles on surface. So far only known from eastern Asia (China, Japan, Korea, Nepal, eastern Russia, and Vietnam).

Tomocerus changbaishanensis Wang

Figs. 3A, 4; Table 1

Tomocerus changbaishanensis Wang, 1999: 177, figs. 1–8, table 1.

Type locality. CHINA, Jilin Province, Changbai Mountain.

Description. ***Size and colouration***: Body length 3.2–4.7 mm. General background colouration of body yellowish white to yellow, head and appendages usually darker yellow. Ant. I and Ant. II antero-laterally with purple patches; Ant III gradually darker towards apex, Ant. IV dark purple. Eye patches black, purple pigment on clypeus and around base of antennae. Lateral side of Th. I and antero-lateral side of front coxa and subcoxa with purple patches, middle coxa and subcoxa occasionally with light purple pigment (Fig. 3A). ***Head***: Antenna 0.95–1.2× length of body. Length ratio of Ant I : II : III : IV = 1.0 : 1.4– 1.6 : 10.9–13.0 : 0.9–1.1. Ant. III basally scaled. PAO absent. Eyes 6+6. Dorsal and ventral sides of head scaled. Cephalic dorsal macrochaetotaxy: anterior area: 2, 4; interocular area: 2, 7, central unpaired macrochaeta present; postocular area: 2+2; posterior area: 3+3. Posterior margin of head with approximately 40+40 small chaetae (Fig. 4A). ***Body chaetotaxy*** (Fig. 4B): Th. II with a file of macrochaetae behind anterior margin. Number of macrochaetae or large mesochaetae in posterior row as 3, 3/ 3, 3, 4, 2, 4 from Th. II to Abd. V. Th. II with six central macrochaetae, inner five arranged approximately in triangular pattern, postero-central macrochaeta near pseudopore; Th. III with anterior macrochaeta; Abd. III with two anterior macrochaetae; Abd. IV with one antero-lateral macrochaeta; Abd. VI with numerous chaetae of different sizes. ***Legs***: Front, middle and hind tibiotarsi ventrally with 6–7, 8–9, 8–9 spine-like chaetae. Tenent hair clavate on all legs, 1.5× length of inner edge of unguis; accessory chaetae small, subequal to pretarsal chaetae; guard chaetae about 0.67× length of tenent hair. Unguis slender, with baso-internal ridges about 1/3 distance from base; lateral teeth pointed, of moderate size. Inner edge of unguis with small basal tooth and 4–6 more distal teeth, sub-basal tooth strongest. Unguiculus lanceolate, about 0.6–0.8× length of unguis, its inner edge with 1–2 small teeth (Fig. 4C). ***Abdominal appendages***: Ventral tube scaled on both faces, anterior face with about 50 chaetae on each side, posterior face with about 140 chaetae, each lateral flap with about 120 chaetae and unscaled. Anterior face of tenaculum with approximately 15 chaetae and 3–5 scales. Ratio manubrium : dens : mucro = 3.8–4.2 : 5.1–5.8 : 1.0. Manubrium ventrally scaled without chaetae; laterally with large round scales and 10–11 chaetae, proximal chaeta small, distal chaetae strong; each dorsal chaetal strip with about 250–350 chaetae of different sizes, each strip with a blunt prominent macrochaeta distally, an irregular row of scales along inner edge and 11–15 pseudopores on lateral side (Fig. 4D); external corner chaeta as large as moderate-size mesochaetae in chaetal strip (Fig. 4E). Dental spine formula as 4–5/3–5, **2**; all spines basally with crown of moderate to large denticles, distally with longitudinal ribs (Fig. 4F). Dens dorsally with ordinary chaetae and plumose chaetae, ventrally densely scaled. Mucronal outer basal tooth with toothlet, apical tooth subequal to subapical tooth, outer lamella with 4–7 intermediate teeth (Fig. 4G).

Differential diagnosis. Compared to most other species of *ocreatus* complex, *T. changbaishanensis* shows an uneven distribution of secondary denticles on dental spines, which appears to be an intermediate form between compound and multi-furcate types. The species is also remarkable for the presence of only one pair of blunt prominent dorsal chaetae on the distal part of manubrium, but not on the basal part of dens. *Tomocerus changbaishanensis* is similar to *Tomocerus deogyuensis* Lee, 1975 in the general appearance, the manubrial blunt chaetae and the large denticles around the base of dental spines, but in the latter species the distal half of the spine is "serrated" with numerous tiny denticles (Lee 1975), while in the former species the distal part of spine is "smooth" with fine longitudinal ribs and only occasionally a few small denticles; in *T. changbaishanensis* the furca ratio is about 4 : 5.5 : 1, and the mucro is about 1.5× length of manubrial prominent chaeta, while in *T. deogyuensis* the furca ratio is 8 : 9 : 1, and the mucro is as long as manubrial prominent chaeta (Lee 1975); *T. deogyuensis* has more (8–11) mucronal intermediate teeth than *T. changbaishanensis* (4–7, average 5); in *T. deogyuensis* purple pigment is on antennae and on tibiotarsi (Lee 1975), while in *T. changbaishanensis* it is also on clypeus, antennal bases and front leg bases, but is not on tibiotarsi.

Habitat and distribution. Frequent in the litter layer of the mixed conifer-broadleaf forest in Changbai Moun-

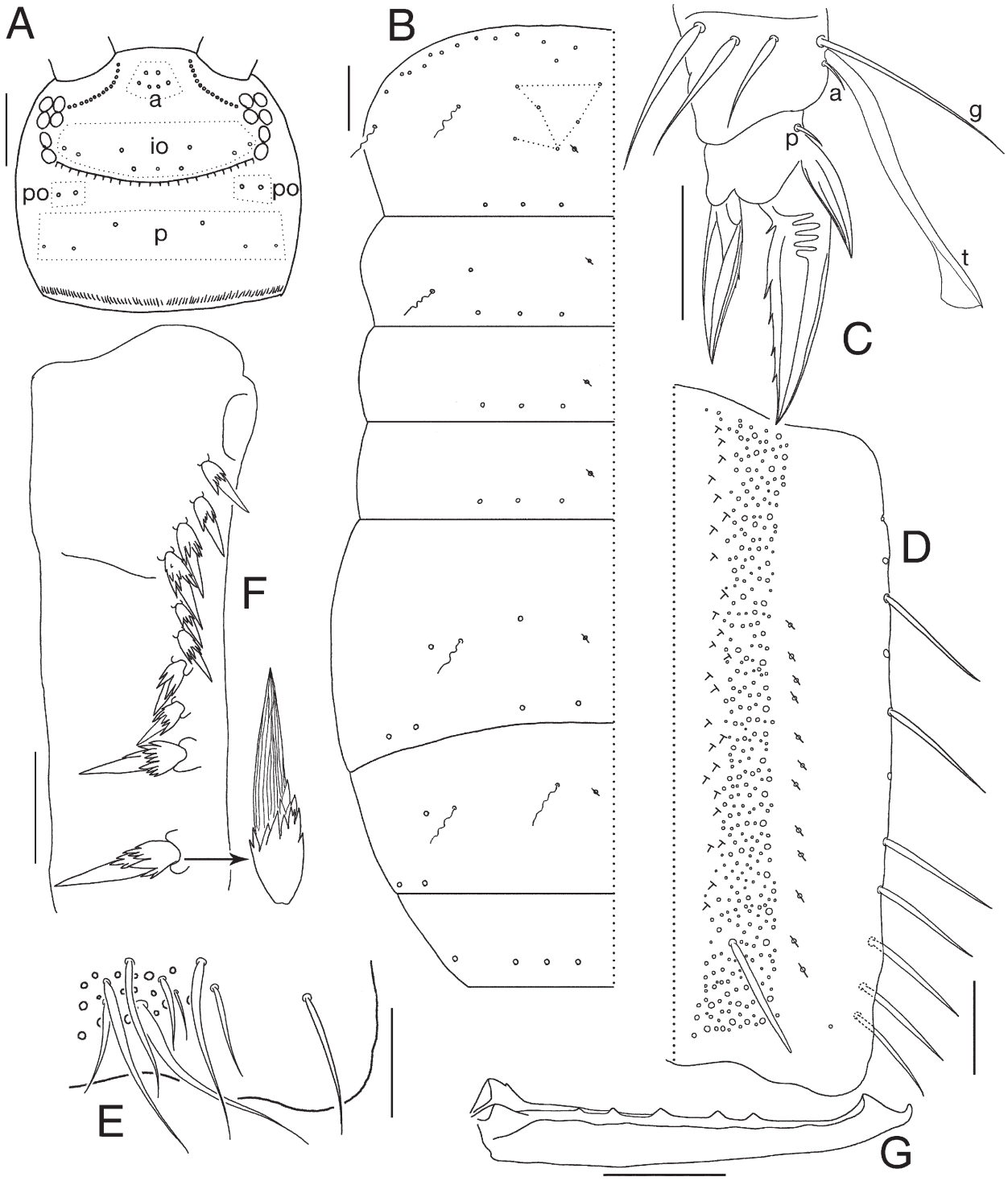

Fig. 4. *Tomocerus changbaishanensis* Wang, 1999. **A**: Cephalic dorsal chaetotaxy, dorsal view; open circle: socket of chaeta, same as below; a: anterior area, io: interocular area, po: postocular area, p: posterior area. **B**: Dorsal chaetotaxy of Th. II–Abd. V, dorsal view; open circle with a slash: pseudopore, wavy line: bothriotricha, same as below. **C**: Hind claw, lateral view; showing chaetae on only one side; t: tenent hair, a: accessory chaeta, g: guard chaeta, p: pretarsal chaeta, same as below. **D**: Right side of manubrium, dorsal view; showing lateral chaetae and prominent dorsal chaetae, same as below. **E**: Disto-external corner of manubrium, dorsal view. **F**: Dental spines, dorsal view; magnified spine showing fine structure, same as below. **G**: Mucro, inner view. (Scale bars: A, B = 200 µm; C, E, G = 50 µm; D, F = 100 µm)

tain. The species is so far the only known representative of the *ocreatus* complex in Northeast China.

Material. Topotypes, 2 ♂ and 1 ♀ on slides, '15CBS6 1–3 | *Tomocerus changbaishanensis*', (NJAU), CHINA, Jilin Province, Baishan, Fusong County, Songjianghe Town, Changbai Mountain, N41°51′27.58″ E127°44′54.28″, 955 m, 23.v.2015, Feng Zhang leg. — Other material. 2 ♀ and 2 ♂ on slides, 'C9600 1–4 | *Tomocerus changbaishanensis*', (NJAU), CHINA, Jilin Province, Yanbian, Antu County, Erdaobaihe Town, near west gate of Changbai Mountain National Forest Park, 24.vii.2009, Jianxiu Chen, Feng Zhang & Daoyuan Yu leg.

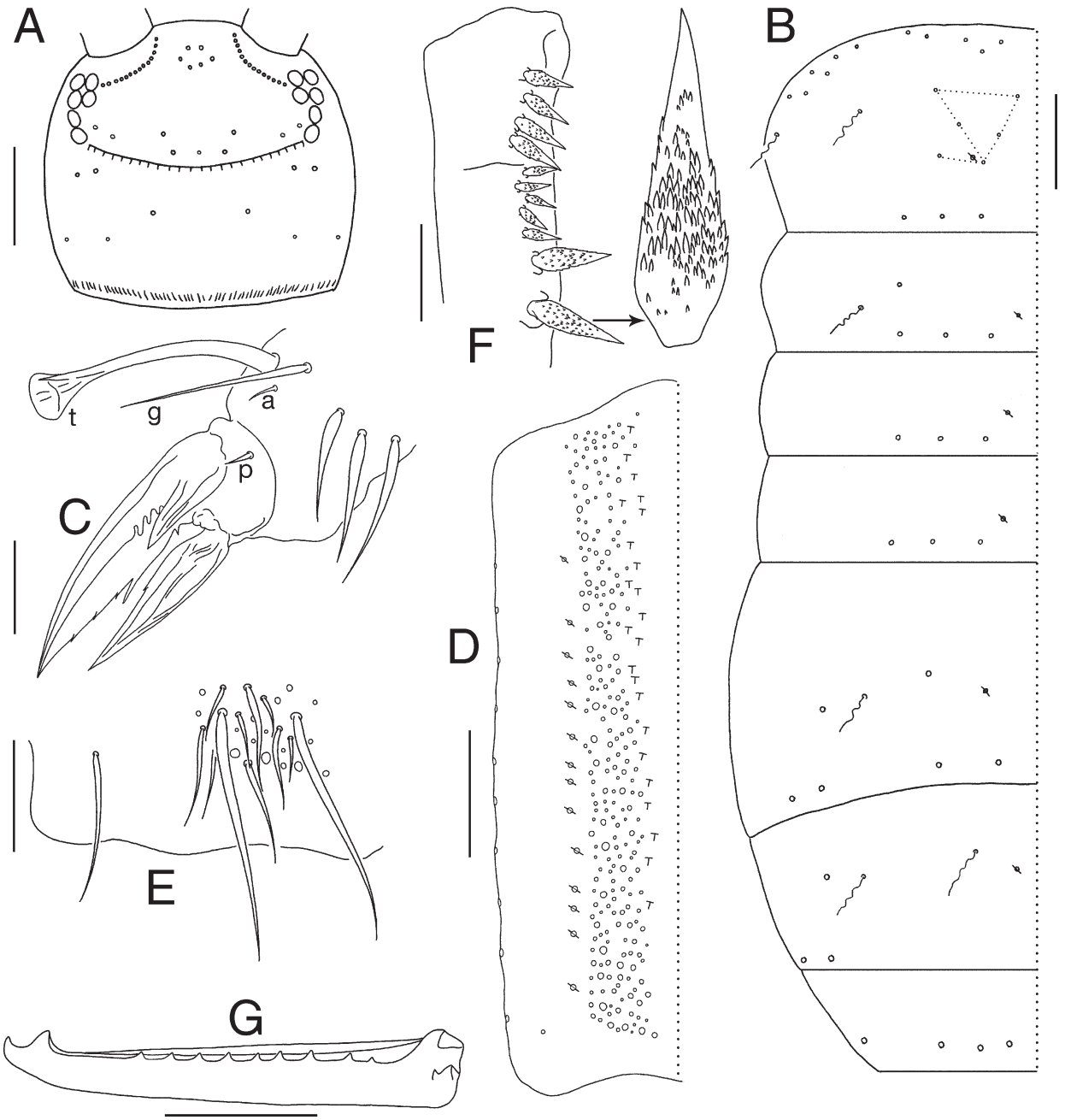

Fig. 5. *Tomocerus huangi* sp.n. **A**: Cephalic dorsal chaetotaxy, dorsal view. **B**: Dorsal chaetotaxy of Th. II–Abd. V, dorsal view. **C**: Hind claw, lateral view. **D**: Left side of manubrium, dorsal view. **E**: Disto-external corner of manubrium, dorsal view. **F**: Dental spines, dorsal view. **G**: Mucro, outer view. (Scale bars: A, B = 200 μm; C, E, G = 50 μm; D, F = 100 μm)

***Tomocerus huangi* Yu sp.n.**

Figs. 3B, 5; Table 1

Description. ***Size and colouration***: Body length 2.5–3.8 mm. General background colouration of body pale yellowish white. Ant. I and Ant. II antero-laterally with dark purple patches, Ant III gradually darker towards apex, Ant. IV dark purple. Clypeus with light purple pigment. Eye patches black, purple pigment behind eye patch. Tibiotarsi with diffuse purple pigment, gradually darker towards apex (Fig. 3B). ***Head***: Antenna 0.97–1.1 × length of body. Length ratio of Ant I : II : III : IV = 1.0 : 1.4–1.5 : 12.4–13.0 : 1.1–1.3. Ant. III basally either with or without scales. PAO absent. Eyes 6+6. Dorsal and ventral sides of head scaled. Cephalic dorsal macrochaetotaxy: anterior area: 2, 4; interocular area: 2, 7, central unpaired macrochaeta present; postocular area: 2+2; posterior area: 3+3. Posterior margin of head with approximately 50+50 small chaetae (Fig. 5A). ***Body chaetotaxy*** (Fig. 5B): Th. II with a file of macrochaetae behind anterior margin. Number of macrochaetae or large mesochaetae in posterior row as 3, 3/ 3, 3, 4, 2, 4 from Th. II to Abd. V. Th. II with six central macrochaetae, inner five arranged approximately in triangular pattern, postero-central macrochaeta near pseudopore; Th. III with

anterior macrochaeta; Abd. III with two anterior macrochaetae; Abd. IV with one antero-lateral macrochaeta; Abd. VI with numerous chaetae of different sizes. ***Legs***: Front, middle and hind tibiotarsi ventrally with 5–6, 6, 7 spine-like chaetae. Tenent hair clavate on all legs, 1.1–1.2× length of inner edge of unguis; accessory chaetae small, thinner than pretarsal chaetae; guard chaetae about 0.75× length of tenent hair. Unguis slender, with baso-internal ridges about 1/3 distance from base; lateral teeth pointed, of moderate size. Inner edge of unguis with small basal tooth and 4–5 more distal teeth, sub-basal tooth very strong. Unguiculus lanceolate, 0.56–0.88× length of unguis, its inner edge with 1 small tooth (Fig. 5C). ***Abdominal appendages***: Ventral tube scaled on both faces, anterior face with 40–50 chaetae on each side, posterior face with 160–180 chaetae, each lateral flap with 140–160 chaetae and 2–5 scales. Anterior face of tenaculum with 2–5 chaetae and without scales. Ratio manubrium : dens : mucro = 3.4–3.6 : 4.4–4.7 : 1.0. Manubrium ventrally scaled without chaetae; laterally with large round scales and 10–11 chaetae, proximal chaeta small, distal chaetae strong; each dorsal chaetal strip with approximately 240 chaetae of different sizes, without distinct prominent chaetae, with an irregular row of scales along inner edge and 10–14 pseudopores on lateral side (Fig. 5D); external corner chaeta as large as moderate-size mesochaetae in chaetal strip (Fig. 5E). Dental spine formula as 4/4–5, **2**; all spines with almost evenly distributed numerous small denticles (Fig. 5F). Dens dorsally with ordinary chaetae and plumose chaetae, ventrally with dense scales. Mucronal outer basal tooth with toothlet, apical tooth subequal to subapical tooth, outer lamella with 3–9 intermediate teeth (Fig. 5G).

Differential diagnosis. *Tomocerus huangi* sp.n. is similar to *T. zayuensis* in the chaetotaxy and structure of the dental spines, but differs from the latter in the pale leg bases, the outstanding sub-basal tooth on unguis, fewer chaetae on the tenaculum, the narrower dorsal scale bands and no distinct prominent chaetae on manubrium. In small individual (< 3 mm) the sub-basal ungual tooth is less outstanding, but is still distinctly larger than other teeth.

Habitat and distribution. In leaf litter of mixed conifer-broadleaf forest. This species was known from the northern area of Guangdong Province, south China. The sympatric distribution of *T. huangi* sp.n., *T. virgatus* sp.n., *T.* cf. *similis* and two other undescribed species of *Tomocerus* suggests the genus is also diversified in the southern mountains of China.

Etymology. Named after Mr. Fusheng Huang in Institute of Zoology, Chinese Academy of Sciences, who was the pioneer of the taxonomy of Chinese Tomoceridae.

Material. Holotype ♀ on slide, 'C9641 1 | *Tomocerus huangi* | holotype', (NJAU), CHINA, Guangdong Province, Nanling Natural Reserve, N24°55′ E113°2′5″, 1050 m, 22.viii.2010, Feng Zhang & Zhaohui Li leg. — Paratypes, 4 ♀ on slides, 'C9641 2–3 | *Tomocerus huangi* | paratype' and 'C9641 4–5 | *Tomocerus huangi* | paratype', 5 in alcohol, 'C9641'–'C9642', (NJAU), same data as holotype.

***Tomocerus pseudocreatus* Yu sp.n.**

Figs. 3C, 6; Table 1

Description. ***Size and colouration***: Body length 2.8–3.5 mm. General background colouration of body white to light yellow. Ant. I and Ant. II antero-laterally with dark purple pigment; Ant III and Ant. IV dark purple. Eye patches black, purple pigment around base of antennae and behind eyes. Clypeus and antero-lateral corner of Th. II occasionally with very light purple pigment. Tibiotarsi with purple pigment (Fig. 3C). ***Head***: Antenna 0.8–1.0× length of body. Length ratio of Ant I : II : III : IV = 1.0 : 1.4–1.6 : 8.5–11.8 : 1.0–1.7. Ant. III basally scaled. PAO absent. Eyes 6+6. Dorsal and ventral sides of head scaled. Cephalic dorsal macrochaetotaxy: anterior area: 2, 4; interocular area: 2, 7, central unpaired macrochaeta present; postocular area: 2+2; posterior area: 2+2. Posterior margin of head with approximately 30+30 small chaetae (Fig. 6A). ***Body chaetotaxy*** (Fig. 6B): Th. II with a file of macrochaetae behind anterior margin. Number of macrochaetae or large mesochaetae in posterior row as 3, 3/ 3, 3, 4, 2, 4 from Th. II to Abd. V. Th. II with 5 central macrochaetae arranged approximately in triangular pattern, postero-central macrochaeta near pseudopore; Th. III with anterior macrochaeta; Abd. III with two anterior macrochaetae; Abd. IV with one antero-lateral macrochaeta; Abd. VI with numerous chaetae of different sizes. ***Legs***: Front, middle and hind tibiotarsi ventrally with 5–6, 5–6, 6–7 strong chaetae, 1, 3–4, 4–5 spine-like. Tenent hair clavate on all legs, subequal to or slightly longer than inner edge of unguis; accessory chaetae small, slightly weaker than pretarsal chaetae; guard chaetae subequal to tenent hair in length. Unguis slender, with baso-internal ridges about 1/3 distance from base; lateral teeth pointed, of moderate size. Inner edge of unguis with basal tooth and 5 more distal teeth, sub-basal tooth slightly stronger. Unguiculus lanceolate, about 0.66× length of unguis, its inner edge with 1 small tooth (Fig. 6C). ***Abdominal appendages***: Ventral tube scaled on both faces, anterior face with about 20 chaetae on each side, posterior face with 60–90 chaetae, each lateral flap with 50–70 chaetae and unscaled. Anterior face of tenaculum with 5–10 chaetae and without scales. Ratio manubrium : dens : mucro = 3.4–3.5 : 4.4–4.6 : 1.0. Manubrium ventrally scaled without chaetae; laterally with large round scales and 9–11 chaetae, proximal chaeta small, distal chaetae strong; each dorsal chaetal strip with approximately 170 chaetae of different sizes and 13–15 pseudopores on lateral side, without scales along inner edge; blunt prominent chaetae 2+2, proximal pair at middle and distal pair near distal end of manubrium (Fig. 6D); external corner chaeta as large as moderate-size mesochaetae in chaetal strip (Fig. 6E). Dens basally with blunt prominent chaeta. Dental spine formula as 3–4/2–3, **2**; all spines with numerous moderate-size denticles (Fig. 6F). Dens dorsally with ordinary chaetae and plumose chaetae, ventrally with dense scales and

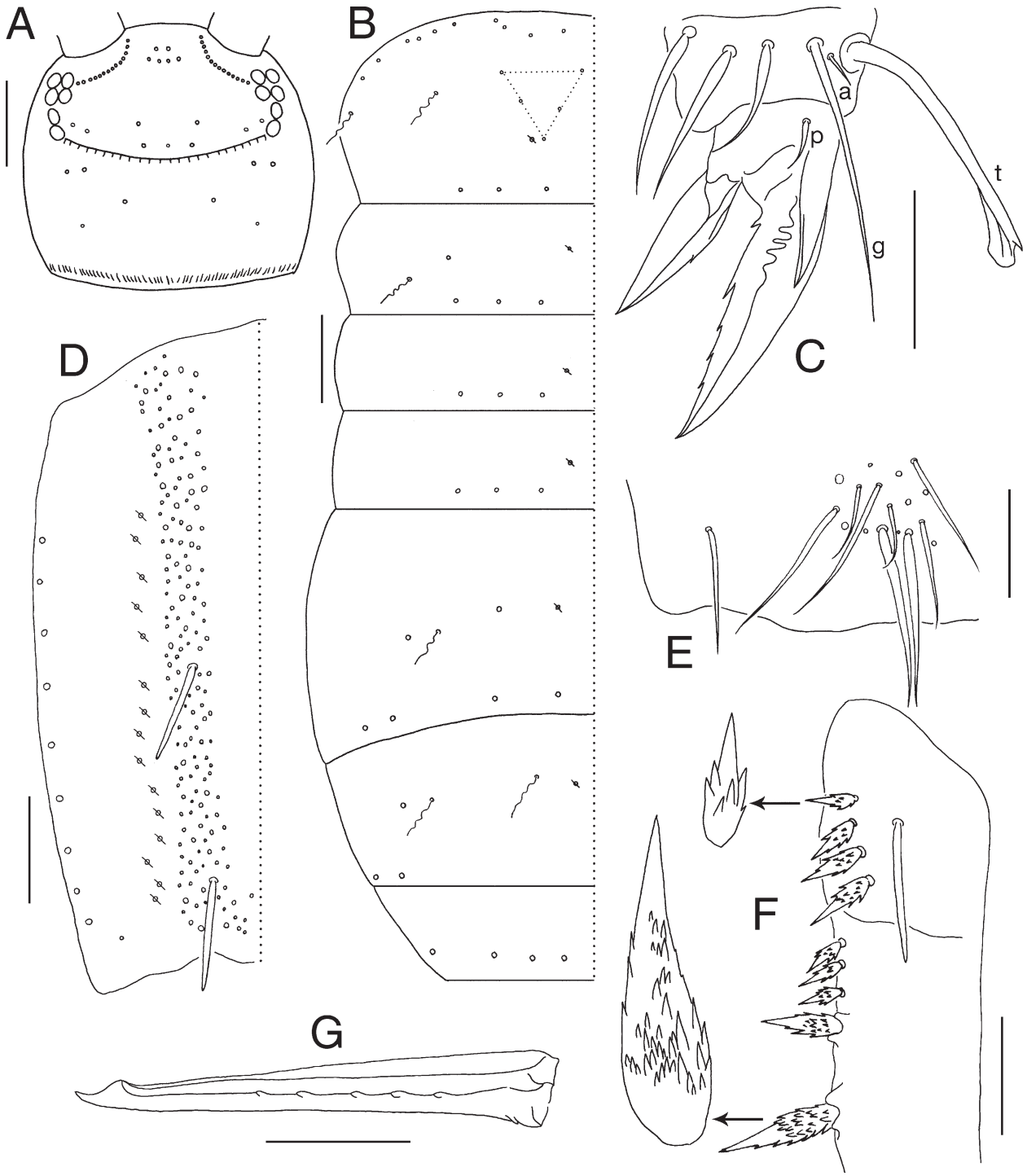

Fig. 6. *Tomocerus pseudocreatus* sp.n. **A**: Cephalic dorsal chaetotaxy, dorsal view. **B**: Dorsal chaetotaxy of Th. II–Abd. V, dorsal view. **C**: Middle claw, lateral view. **D**: Right side of manubrium, dorsal view. **E**: Disto-external corner of manubrium, dorsal view. **F**: Spines and prominent dorso-basal chaeta on dens, dorsal view. **G**: Mucro, dorsal view. (Scale bars: A, B = 200 µm; C, E, G = 50 µm; D, F = 100 µm)

several apical chaetae. Mucronal outer basal tooth with toothlet, apical tooth subequal to subapical tooth, outer lamella with 5–6 intermediate teeth (Fig. 6G).

Differential diagnosis. *Tomocerus pseudocreatus* sp.n. is similar to *T. ocreatus* and *T. yueluensis* sp.n. in the absence of dorsal manubrial scales and the shape and arrangement of dental spines, but can be distinguished from both species in the presence of 2+2 blunt prominent chaetae on manubrium and 1+1 on dens. Besides, *T. pseudocreatus* sp.n. differs from *T. ocreatus* mainly in the patterns of cephalic and mesothoracic macrochaetotaxy, and differs from *T. yueluensis* sp.n. in the absence of lateral pigment bands on thoracic terga.

Habitat and distribution. Generally found in leaf litter and rotted wood, also on trunk of *Liquidambar formosana* in sample C9671. The species is rather common in the mountain areas around the border between Anhui and Jiangxi Provinces, southeast China.

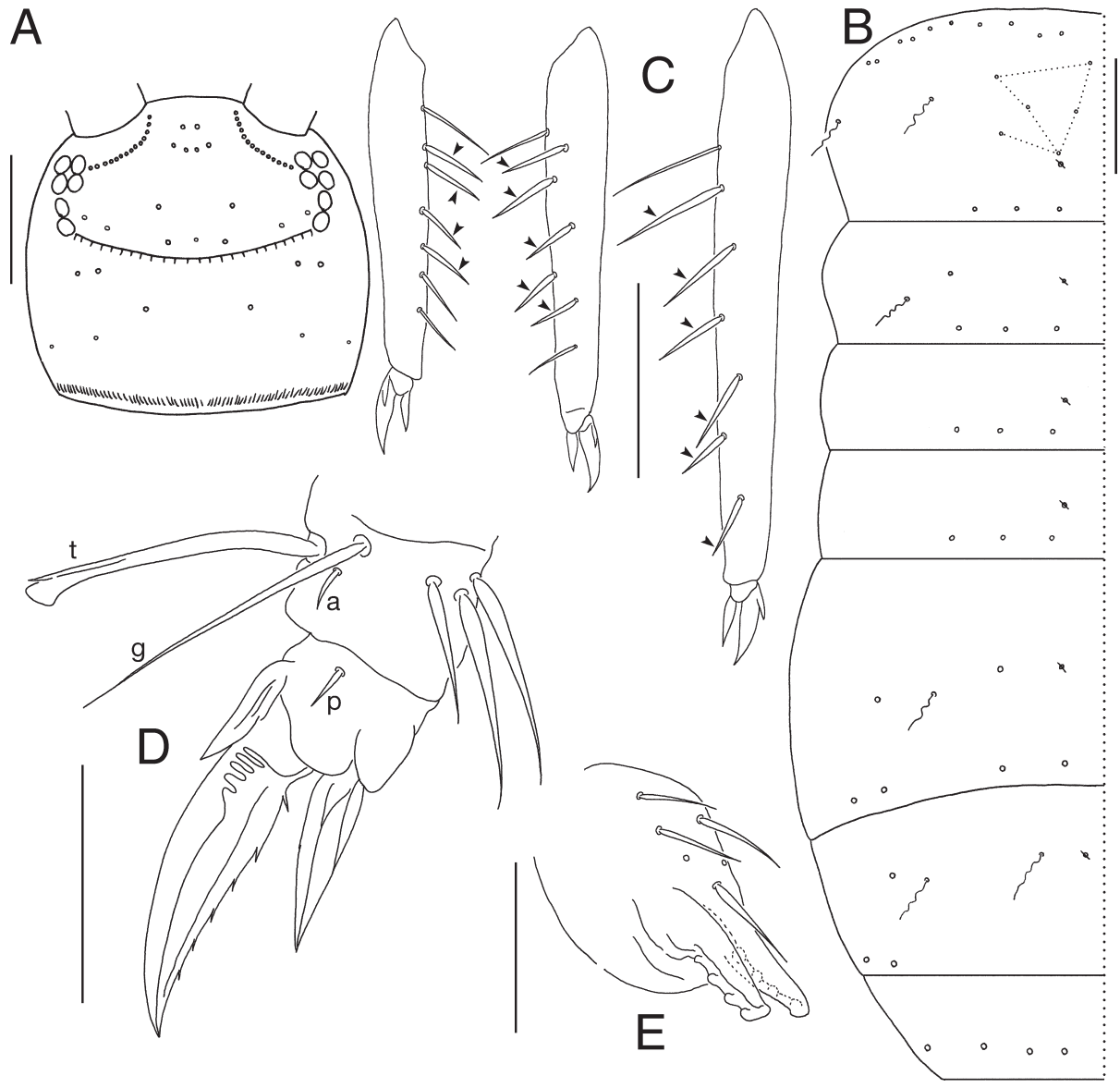

Fig. 7. *Tomocerus spinulus* Chen & Christiansen, 1998. **A**: Cephalic dorsal chaetotaxy, dorsal view. **B**: Dorsal chaetotaxy of Th. II–Abd. V, dorsal view. **C**: Tibiotarsi, lateral view; showing strong inner chaetae, arrows pointing to spine-like ones, same as below. **D**: Front claw, lateral view. **E**: Tenaculum, anterior view. (Scale bars: A, B, C = 200 μm; D, E, G = 50 μm)

Etymology. Combination of the Greek word *pseudo*: false, and the specific name of the related species *T. ocreatus*.

Material. Holotype ♂ on slide, 'C9671 1 | *Tomocerus pseudocreatus* | holotype', (NJAU), CHINA, Anhui Province, Qimen County, Likou Town, Lixi Village, N29°59′14.46″ E117°29′13.44″, 225 m, 12.viii.2011, Feng Zhang, Daoyuan Yu & Yuanhao Ren leg. — Paratypes, 2 ♀ on slides, 'C9671 2–3 | *Tomocerus pseudocreatus* | paratype', 3 in alcohol, 'C9671', (NJAU), same data as holotype. — Other material. 1 ♂ and 1 ♀ on slides, '15WY3 1–2 | *Tomocerus pseudocreatus*', 10 in alcohol, '15WY3', (NJAU), CHINA, Jiangxi Province, Shangrao, Wuyuan County, N29°14′50.96″ E117°50′59.22″, 93 m, 9.ix.2015, Feng Zhang and Daoyuan Yu leg.; 1 ♀ on slide, 'S4383 | *Tomocerus pseudocreatus*', 2 in alcohol, 'S4383', (NJAU), CHINA, Jiangxi Province, Nanchang, Fengjing Village, N28°47′30″ E115°48′27″, 138 m, 11.viii.2012, Zhixiang Pan leg.; 1 ♀ on slide, 'S4386 | *Tomocerus pseudocreatus*', (NJAU), CHINA, Jiangxi Province, Jiujiang, Lu Mountain, Bilong Lake, N29°35′45″ E116°2′27″, 172 m, 12.viii.2012, Zhixiang Pan leg.; 1 ♀ on slide, 'S4387 | *Tomocerus pseudocreatus*', 3 in alcohol, 'S4387', (NJAU), CHINA, Jiangxi Province, Jiujiang, South Lake Park, N29°42′42″ E115°59′54″, 25 m, 12.viii.2012, Zhixiang Pan leg.

Tomocerus spinulus Chen & Christiansen

Figs. 3D, 7, 8; Table 1

Tomocerus spinulus Chen & Christiansen, 1998: 51, figs. 1–17, tables 1, 2.

Type locality. CHINA, Anhui Province, Yellow Mountain.

Description. ***Size and colouration***: Body length 2.5–3.1 mm. General background colouration of body light to brownish yellow. Ant. I and Ant. II with diffuse purple pigment; Ant. III gradually darker from base to apex;

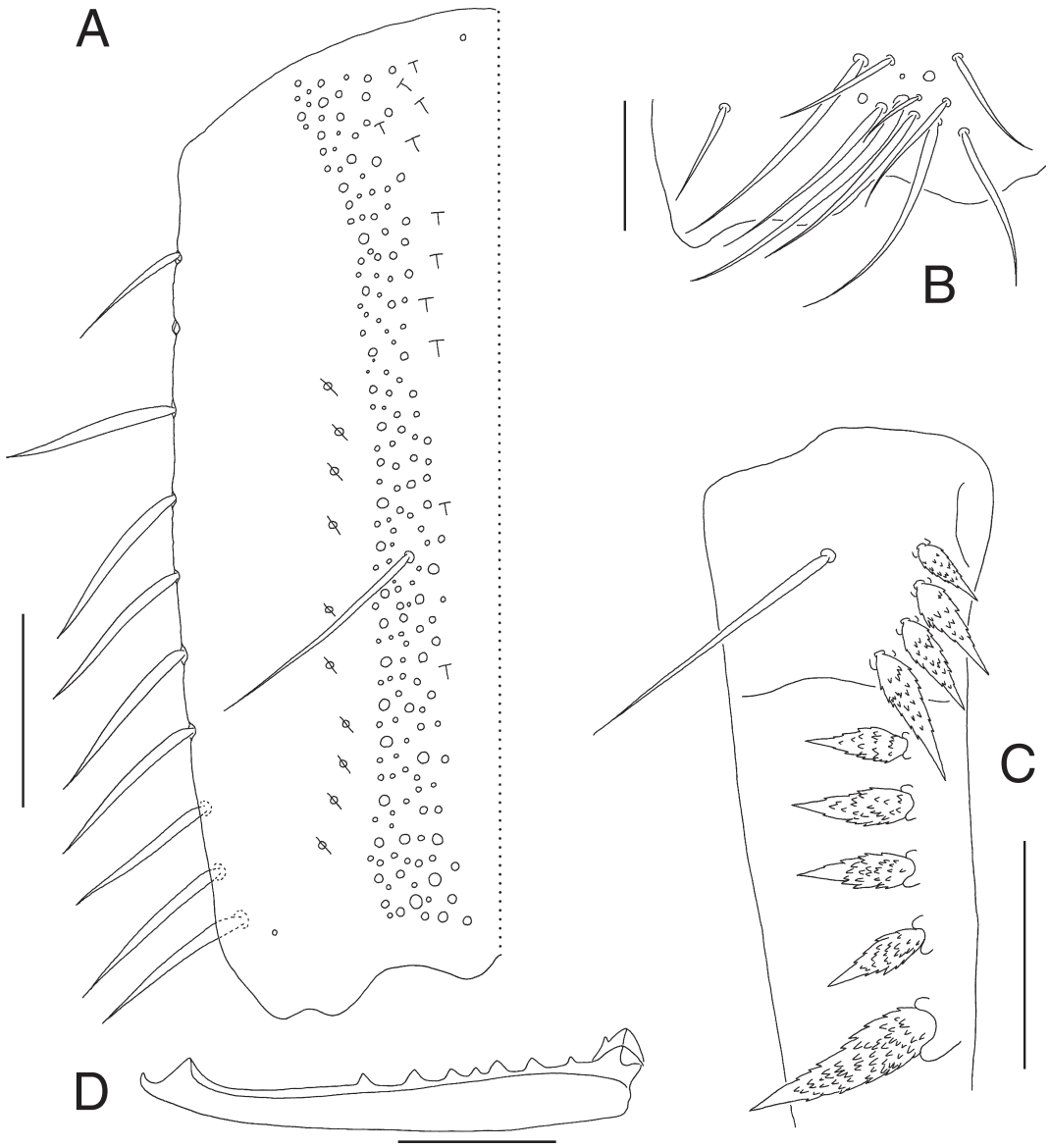

Fig. 8. *Tomocerus spinulus* Chen & Christiansen, 1998. **A**: Left side of manubrium, dorsal view. **B**: Disto-external corner of manubrium, dorsal view. **C**: Spines and prominent dorso-basal chaeta on dens, dorsal view. **D**: Mucro, inner view. (Scale bars: A, C = 100 µm; B, D = 50 µm)

Ant. IV dark purple. Eye patches black, purple pigment around base of antennae and behind eye patches. Leg bases and tibiotarsi with purple pigment (Fig. 3D). ***Head***: Antenna short, 0.58–0.63 × length of body. Length ratio of Ant I : II : III : IV = 1.0 : 1.2–1.4 : 6.9–7.9 : 0.9–1.1. Ant. III baso-laterally with several scales. PAO absent. Eyes 6+6. Dorsal and ventral sides of head scaled. Cephalic dorsal macrochaetotaxy: anterior area: 2, 4; interocular area: 2, 7, central unpaired macrochaeta present; postocular area: 2+2; posterior area: 3+3. Posterior margin of head with approximately 35+35 small chaetae (Fig. 7A). ***Body chaetotaxy*** (Fig. 7B): Th. II with file of macrochaetae behind anterior margin. Number of macrochaetae or large mesochaetae in posterior row as 3, 3/3, 3, 4, 2, 4 from Th. II to Abd. V. Th. II with six central macrochaetae, inner five arranged approximately in triangular pattern, postero-central macrochaeta near pseudopore; Th. III with anterior macrochaeta; Abd. III with two anterior macrochaetae; Abd. IV with one antero-lateral macrochaeta; Abd. VI with numerous chaetae of different sizes. ***Legs***: Front, middle and hind tibiotarsi ventrally with 7, 7, 7 strong chaetae, 4, 4–5, 6 spine-like (Fig. 7C). Tenent hair clavate on all legs, as long as inner edge of unguis; accessory chaetae small, subequal to or slightly weaker than pretarsal chaetae; guard chaetae subequal to or slightly longer than tenent hair. Unguis slender, with baso-internal ridges about 1/3 distance from base; lateral teeth pointed, of small to moderate size. Inner edge of unguis with distinct basal tooth and 4–5 more distal teeth. Unguiculus lanceolate, about 0.6–0.75 × length of unguis, its inner edge with one minute tooth (Fig. 7D). ***Abdominal appendages***: Ventral tube scaled on both faces. Anterior face with 15–25 chaetae on each side, posterior face with 55–70 chaetae, each lat-

eral flap with 50–70 chaetae. Anterior face of tenaculum with 4–12 chaetae and without scales (Fig. 7E). Ratio manubrium : dens : mucro = 2.9–3.2 : 3.5–3.8 : 1.0. Manubrium ventrally scaled without chaetae; laterally with large round scales and 10 chaetae, proximal 1–2 chaetae small, distal chaetae strong; each dorsal chaetal strip with approximately 180 chaetae of different sizes, an irregular row of scales from base to about 2/3 length of manubrium along inner edge and 10 pseudopores on lateral side; prominent chaetae 1+1, slender and pointed, at 1/2–3/5 length from base of manubrium (Fig. 8A); external corner chaeta as large as small mesochaetae in chaetal strip (Fig. 8B). Dens basally with prominent pointed dorsal chaeta. Dental spine formula as 3–5/3–5, **1**; all spines with almost evenly distributed numerous small denticles (Fig. 8C). Dens dorsally with ordinary chaetae and plumose chaetae, ventrally with dense scales and a few apical chaetae. Mucronal outer basal tooth with toothlet, apical tooth subequal to subapical tooth, outer lamella with 3–7 intermediate teeth (Fig. 8D).

Differential diagnosis. Among the *ocreatus* complex, *T. spinulus* is characterized by the short antennae and by the presence of only one large distal dental spine. In addition, it has only 1+1 slender pointed prominent chaetae on manubrium, which is also different from other known species. The denticles on dental spines are generally small, but some moderate-size denticles are occasionally present on some spines, especially on the small spines.

Habitat and distribution. Found in mixed conifer-broadleaf litter and in humus. The species is so far known only from Yellow Mountain, southeast China.

Material. Holotype ♂ on slide, '8220 | *Tomocerus spinulus* | holotype', (NJAU), CHINA, Anhui Province, Yellow Mountain, 16.vii.1990, Jianxiu Chen leg. — Paratypes, 2 ♂ and 7 ♀ on slides, '8220 | *Tomocerus spinulus* | paratype'(NJAU), same data as holotype. — Topotypes, 3 ♀, 2 ♂ and 1 subadult on slides, '16HS02 1–6 | *Tomocerus spinulus*', 10 in alcohol, '16HS02', (NJAU), CHINA, Anhui Province, Yellow Mountain, N30°4′39″ E118°9′3″, 527 m, 2.iii.2016, Daoyuan Yu leg.

Tomocerus virgatus Yu sp.n.

Figs. 3E, 9; Table 1

Description. ***Size and colouration***: Body length 2.8–3.8 mm. General background colouration of body yellowish white. Ant. I dorsally with dark purple pigment at base and apex; Ant. II distally with diffused purple pigment; Ant. III pale at base and gradually darker towards apex. Eye patches black, purple pigment at base of antenna and behind eyes. Lateral margins of thoracic terga with narrow purple bands. Inner sides of femora and basal parts of tibiotarsi with dark purple bands, apices of tibiotarsi with diffused purple pigment (Fig. 3E). ***Head***: Intact antenna not seen, longest observed reconstructed antennae 1.5–1.6× length of body. Length ratio of Ant I : II : III + IV = 1.0 : 1.7–1.9 : 20.3. Ant. III basally scaled. PAO absent. Eyes 6+6. Dorsal and ventral sides of head scaled. Cephalic dorsal macrochaetotaxy: anterior area: 2, 4; interocular area: 2, 6, central unpaired macrochaeta absent; postocular area: 2+2; posterior area: 2+2, posterior pair smaller. Posterior margin of head with approximately 40+40 small chaetae (Fig. 9A). ***Body chaetotaxy*** (Fig. 9B): Th. II with file of macrochaetae behind anterior margin. Number of macrochaetae or large mesochaetae in posterior row as 3, 3/ 3, 3, 4, 2, 4 from Th. II to Abd. V. Th. II with 1 central macrochaeta distant from pseudopore; Th. III with anterior macrochaeta; Abd. III with two anterior macrochaetae; Abd. IV with one antero-lateral macrochaeta; Abd. VI with numerous chaetae of different sizes. ***Legs***: Each tibiotarsus with 5–7 blunt spine-like inner chaetae. Tenent hair clavate on all legs, longer than inner edge of unguis; accessory chaetae small, slightly weaker than pretarsal chaetae; guard chaetae subequal to tenent hair in length. Unguis slender, with baso-internal ridges about 1/3 distance from base; lateral teeth pointed, of moderate size. Inner edge of unguis with basal tooth and 4 more distal teeth, sub-basal tooth slightly stronger. Unguiculus lanceolate, about 0.75× length of unguis, its inner edge with 1 tooth (Fig. 9C). ***Abdominal appendages***: Ventral tube scaled on both faces, anterior face with 15–20 chaetae on each side, posterior face with 50–60 chaetae, each lateral flap with 45–55 chaetae and unscaled. Anterior face of tenaculum with 5 chaetae, without scales (Fig. 9D). Ratio manubrium : dens : mucro = 3.2–3.4 : 4.4–4.5 : 1.0. Manubrium ventrally scaled without chaetae; laterally with large, round scales and 8–9 chaetae, proximal chaeta small, distal chaetae strong; each dorsal chaetal strip with approximately 120 chaetae of different sizes and 10 pseudopores on lateral side, without dorsal scales and distinct prominent chaetae (Fig. 9E); external corner chaeta as large as moderate-size mesochaetae in chaetal strip (Fig. 9F). Dental spine formula as 4–5/3–4, **2**; all spines with numerous moderate to large denticles covering at least basal 2/3 (Fig. 9G). Dens dorsally with ordinary chaetae and plumose chaetae, ventrally with dense scales and a few apical chaetae. Mucronal outer basal tooth with toothlet, apical tooth subequal to or slightly weaker than subapical tooth, outer lamella with 6 intermediate teeth (Fig. 9H).

Differential diagnosis. *Tomocerus virgatus* sp.n. is characterized by its unique colour pattern, especially the banded femora and tibiotarsi. This species has only one macrochaeta in the central area of Th. II, which separates it from the rest of the *ocreatus* complex except *T. ocreatus* from Vietnam. However, cephalic chaetotaxy differs between the two species. In addition, the relative length of antenna (antenna:body) of *T. virgatus* sp.n. are about 1.5× of that of *T. ocreatus*, and the denticles on dental spines are larger than those in *T. ocreatus*. Some large specimens of the new species have mesonotum slightly projecting over prothorax and posterior margin of head.

Habitat and distribution. In leaf litter of mixed forest and under barks of rotted wood. The species is so far known from northern and central area of Guangdong Province, south China.

Etymology. Named after the banded pattern on the legs. Latin word *virgatus*: banded.

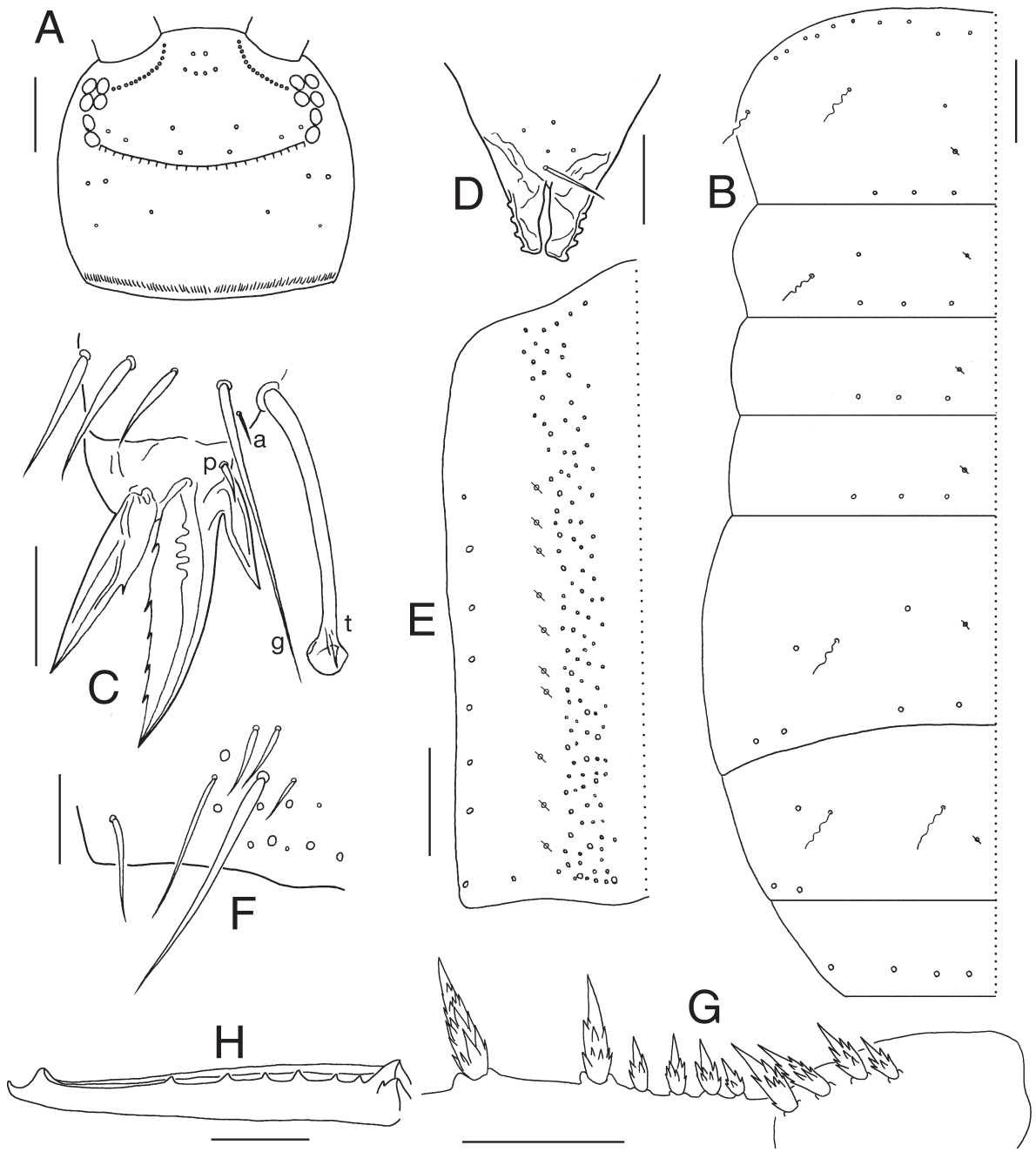

Fig. 9. *Tomocerus virgatus* sp.n. **A**: Cephalic dorsal chaetotaxy, dorsal view. **B**: Dorsal chaetotaxy of Th. II–Abd. V, dorsal view. **C**: Hind claw, lateral view. **D**: Tenaculum, anterior view. **E**: Left side of manubrium, dorsal view. **F**: Disto-external corner of manubrium, dorsal view. **G**: Dental spines, dorsal view. **H**: Mucro, outer view. (Scale bars: A, B = 200 µm; C, D, F, H = 50 µm; E, G = 100 µm)

Material. Holotype ♀ on slide, 'S4149 | *Tomocerus virgatus* | holotype', (NJAU), CHINA, Guangdong Province, Huizhou, Longmen County, Nankunshan Natural Reserve, N23°38′47.27″ E113°50′42.91″, 700–800 m, 22.viii.2010, Zhixiang Pan leg. — Paratypes, 1 ♂ on slide, 'S4147 | *Tomocerus virgatus* | paratype', 2 in alcohol, 'S4147' and 'S4149', (NJAU), same data as holotype. — Other materials, 2 ♂ and 1 ♀ on slides, 'C9641–9642 1–3 | *Tomocerus virgatus*', 2 in alcohol, 'C9641', (NJAU), CHINA, Guangdong Province, Nanling Natural Reserve, N24°55′ E113°2′5″, 1050m, 22.viii.2010, Feng Zhang & Zhaohui Li leg.

***Tomocerus yueluensis* Yu sp.n.**

Figs. 3F, 10, 11; Table 1

Description. ***Size and colouration***: Body length 2.6–3.3 mm. General background colouration of body yellowish white. Ant. I and Ant. II antero-laterally with purple pigment; Ant III+IV gradually darker towards apex. Eye patches black, purple pigment at base of antennae and behind eyes. Antero-lateral margin of Th. II and Th. III with purple patches. Tibiotarsi with diffuse purple pigment (Fig. 3F). ***Head***: Intact antennae not present in collected specimens, longest observed reconstructed

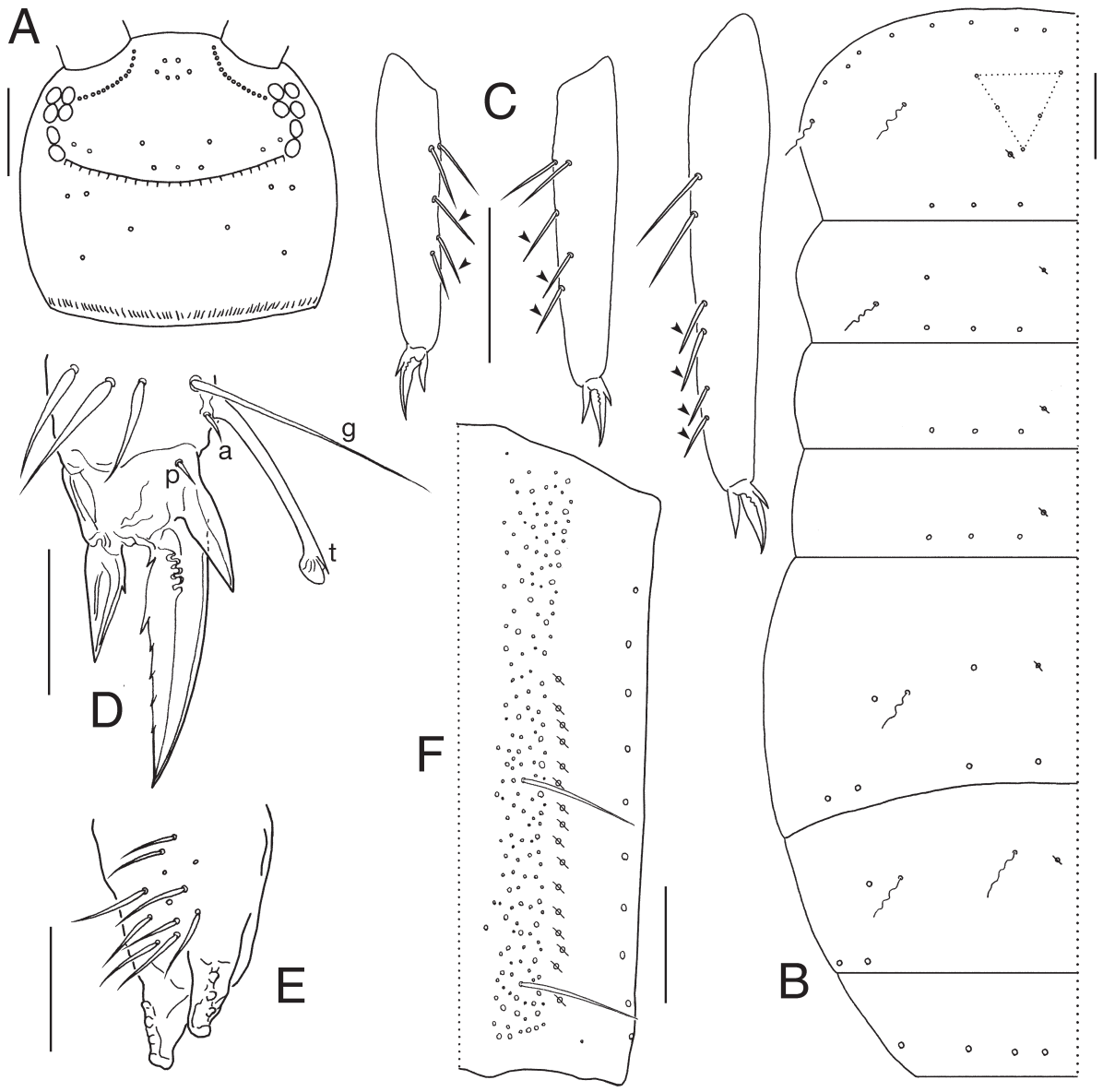

Fig. 10. *Tomocerus yueluensis* sp.n. **A**: Cephalic dorsal chaetotaxy, dorsal view. **B**: Dorsal chaetotaxy of Th. II–Abd. V, dorsal view. **C**: Tibiotarsi, lateral view. **D**: Front claw, lateral view. **E**: Tenaculum, anterior view. **F**: Right side of manubrium, dorsal view. (Scale bars: A, B, C = 200 μm; D, E = 50 μm; F = 100 μm)

antennae about 0.75–0.8× length of body, length ratio as Ant I : II : III+IV = 1.0 : 1.4–1.7 : 8.3–9.5. Ant. III basally with a few scales. PAO absent. Eyes 6+6. Dorsal and ventral sides of head scaled. Cephalic dorsal macrochaetotaxy: anterior area: 2, 4; interocular area: 2, 7, central unpaired macrochaeta present; postocular area: 2+2; posterior area: 2+2. Posterior margin of head with approximately 30+30 small chaetae (Fig. 10A). ***Body chaetotaxy*** (Fig. 10B): Th. II with file of macrochaetae behind anterior margin. Number of macrochaetae or large mesochaetae in posterior row as 3, 3/ 3, 3, 4, 2, 4 from Th. II to Abd. V. Th. II with 5 central macrochaetae arranged approximately in triangular pattern, postero-central macrochaeta near pseudopore; Th. III with anterior macrochaeta; Abd. III with two anterior macrochaetae; Abd. IV with one antero-lateral macrochaeta; Abd. VI with numerous chaetae of different sizes. ***Legs***: Front, middle and hind tibiotarsi ventrally with 5–6, 5–6, 5–7 strong chaetae, 1–2, 2–3, 3–4 spine-like (Fig. 10C). Tenent hair clavate on all legs, subequal to inner edge of unguis in length; accessory chaetae subequal to pretarsal chaetae; guard chaetae slightly longer than tenent hair. Unguis slender, with baso-internal ridges about 1/3 distance from base; lateral teeth pointed, of moderate size. Inner edge of unguis with basal tooth and 5 more distal teeth, subbasal tooth distinctly stronger. Unguiculus lanceolate, about 0.5–0.75× length of unguis, its inner edge with 1 small tooth (Fig. 10D). ***Abdominal appendages***: Ventral tube scaled on both faces, anterior face with about 30–35 chaetae on each side, posterior face with 80–100 chaetae, each lateral flap with 60–80 chaetae and unscaled. Anterior face of tenaculum with approximately 12 chaetae, without scales (Fig. 10E). Ratio manubrium : dens : mucro = 3.3–3.7 : 4.3–4.6 : 1.0. Manubrium ventrally

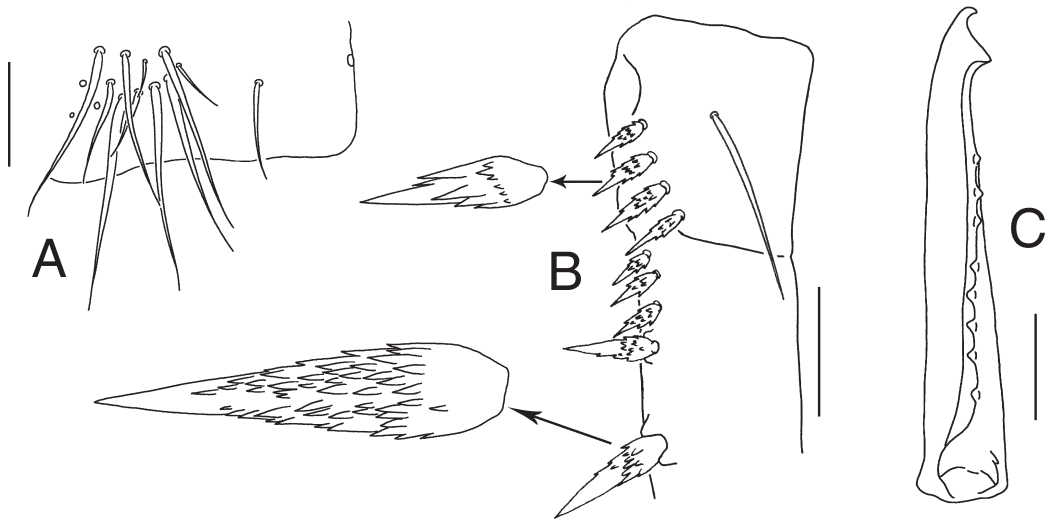

Fig. 11. *Tomocerus yueluensis* sp.n. **A**: Disto-external corner of manubrium, dorsal view. **B**: Spines and prominent dorso-basal chaeta on dens, dorsal view. **C**: Mucro, dorso-inner view. (Scale bars: A, C = 50 μm; B = 100 μm)

scaled without chaetae; laterally with large round scales and 9–11 chaetae, proximal chaeta small, distal chaetae strong; each dorsal chaetal strip with approximately 175 chaetae of different sizes and 15–16 pseudopores on lateral side, without dorsal scales; prominent chaetae 2+2, slender and pointed, proximal prominent chaeta at about 1/2 length from base of manubrium, distal prominent chaeta near distal end of manubrium (Fig. 10F); external corner chaeta as large as small to moderate-size mesochaetae in chaetal strip (Fig. 11A). Dens basally with pointed prominent dorsal chaeta. Dental spine formula as 4–5/2–4, **2**; all spines with numerous moderate-size denticles (Fig. 11B). Dens dorsally with ordinary chaetae and plumose chaetae, ventrally with dense scales and a few apical chaetae. Mucronal outer basal tooth with toothlet, apical tooth subequal to subapical tooth, outer lamella with 7–8 intermediate teeth (Fig. 11C).

Differential diagnosis. *Tomocerus yueluensis* sp.n. is similar to *T. qinae* in the general colour pattern, the chaetotaxy, the claw morphology and the shape and arrangement of dental spines, but differs from the latter in having a smaller body size (about 0.7× of that of *T. qinae*), shorter antenna (value of antenna:body about 0.6–0.7× of that of *T. qinae*), narrower and lighter pigment bands on thoracic terga, and the absence of scales on tenaculum and dorsal side of manubrium. Besides, *T. qinae* has in most cases 6 central macrochaetae on Th. II, while *T. yueluensis* sp.n. has only and constantly the inner 5 of them.

Habitat and distribution. In mixed litter and on rotten wood. The species is so far known only from Yuelu Mountain.

Etymology. Named after the type locality: Yuelu Mountain.

Material. Holotype ♀ on slide, 'S4381 | *Tomocerus yueluensis* | holotype', (NJAU), CHINA, Hunan Province, Changsha, Yuelu Mountain, N28°11′45″ E112°56′40″, 50 m, 9.viii.2012, Zhixiang Pan leg. — Paratypes, 3 ♀ and 1 ♂ on slides, 'S4382 1–4 | *Tomocerus yueluensis* | paratype', (NJAU), same area as holotype, N28°11′34″ E112°56′1″, 244 m.

Tomocerus zayuensis Huang & Yin

Figs. 3G, 12; Table 1

Tomocerus zayuensis Huang & Yin, 1981: 43, figs. 7–8.

Type locality. CHINA, Tibet, Nyingchi, Zayu County.

Description. ***Size and colouration***: Body length 3.3–4.1 mm. General background colouration of body light yellow. Ant. I antero-laterally light purple; Ant II–Ant. IV dark purple. Eye patches black, purple pigment around mouthparts, base of antennae and eye patches. Th. II laterally with a little purple pigment. Leg bases with dark purple patches; tibiotarsi purple, gradually darker towards tips; other leg segments, ventral tube and dorsal side of manubrium with diffused purple pigment (Fig. 3G). ***Head***: Antenna 0.72–0.80× length of body. Length ratio of Ant I : II : III : IV = 1.0 : 1.3–1.5 : 7.4–8.1 : 1.2–1.5. Ant. III basally scaled. PAO absent. Eyes 6+6. Dorsal and ventral sides of head scaled. Cephalic dorsal macrochaetotaxy: anterior area: 2, 4; interocular area: 2, 7, central unpaired macrochaeta present; postocular area: 2+2; posterior area: 3+3. Posterior margin of head with approximately 35+35 small chaetae (Fig. 12A). ***Body chaetotaxy*** (Fig. 12B): Th. II with file of macrochaetae behind anterior margin. Number of macrochaetae or large mesochaetae in posterior row as 3, 3/ 3, 3, 4, 2, 4 from Th. II to Abd. V. Th. II with six central macrochaetae, inner five arranged approximately in triangular pattern, posterocentral macrochaeta near pseudopore; Th. III with anterior macrochaeta; Abd. III with two anterior macrochaetae; Abd. IV with one antero-lateral macrochaeta; Abd. VI with numerous chaetae of different sizes. ***Legs***: Front, middle and hind tibiotarsi ventrally with 6–8, 6–8, 8–10 spine-like chaetae. Tenent hair clavate on all legs,

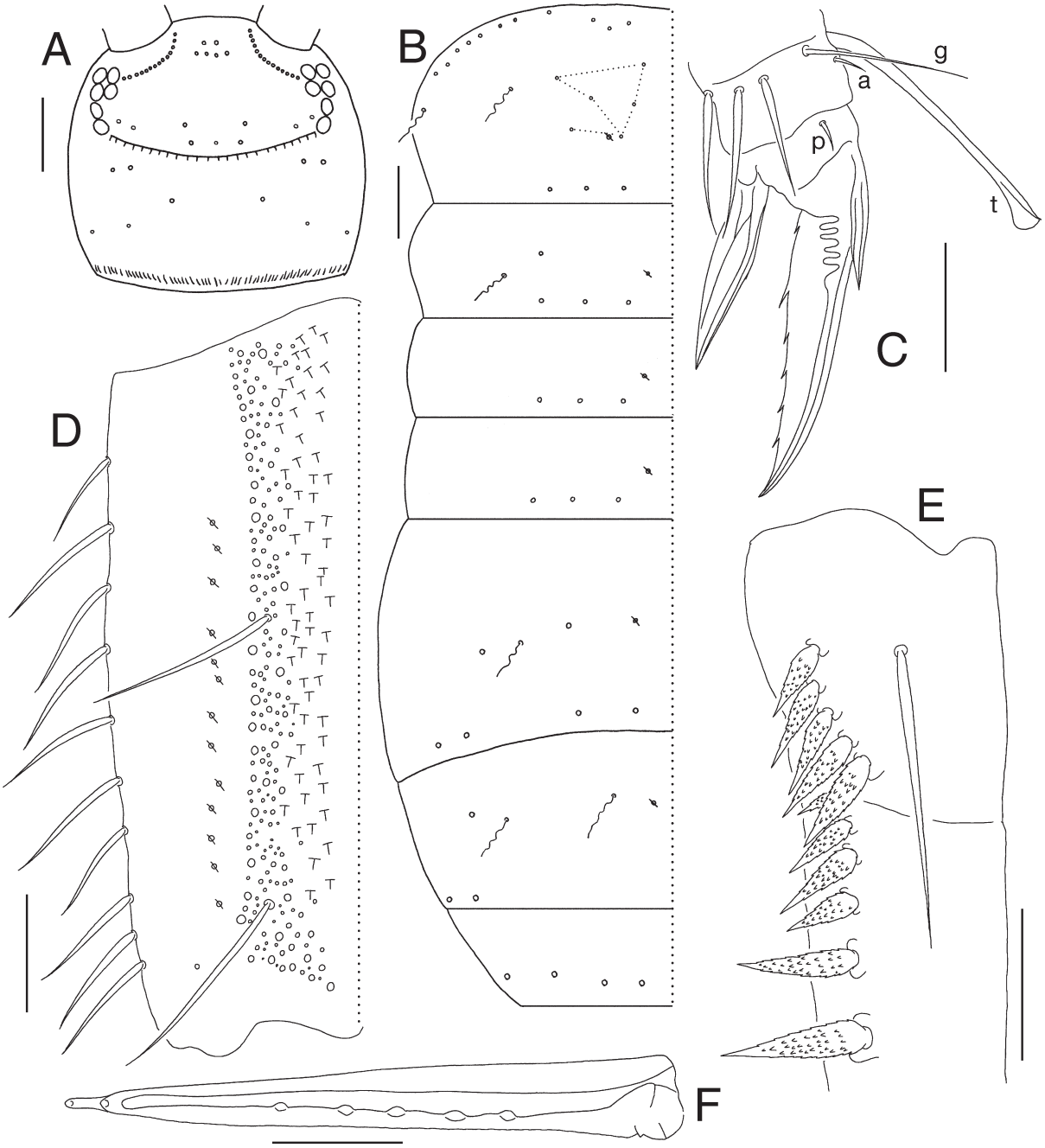

Fig. 12. *Tomocerus zayuensis* Huang & Yin, 1981. **A**: Cephalic dorsal chaetotaxy, dorsal view. **B**: Dorsal chaetotaxy of Th. II–Abd. V, dorsal view. **C**: Hind claw, lateral view. **D**: Left side of manubrium, dorsal view. **E**: Spines and prominent dorso-basal chaeta on dens, dorsal view. **F**: Mucro, dorsal view. (Scale bars: A, B = 200 µm; C, F = 50 µm; D, E = 100 µm)

as long as inner edge of unguis; accessory chaetae small, subequal to pretarsal chaetae; guard chaetae about 0.6× length of tenent hair. Unguis slender, with baso-internal ridges about 1/3 distance from base; lateral teeth pointed, of moderate size. Inner edge of unguis with small basal tooth and 4–6 more distal teeth, sub-basal tooth slightly larger. Unguiculus lanceolate, about 0.6–0.7× length of unguis, its inner edge with 0–1 very minute tooth (Fig. 12C). ***Abdominal appendages***: Ventral tube scaled on both faces, with numerous chaetae of different sizes. Anterior face of tenaculum with approximately 15 chaetae and without scales. Ratio manubrium : dens : mucro = 3.2–3.5 : 4.4–4.7 : 1.0. Manubrium ventrally scaled without chaetae; laterally with large, round scales and 10 chaetae, proximal chaeta small, distal chaetae strong; each dorsal chaetal strip with approximately 200 chaetae of different sizes, dense strip of scales along inner edge and 12–15 pseudopores on lateral side; prominent chaetae 2+2, slender and pointed, proximal prominent chaeta at about 2/5–1/2 × length from base of manubrium, distal prominent chaeta near distal end of manubrium; external corner chaeta as large as moderate-size mesochaetae in chaetal strip (Fig. 12D). Dens basally with pointed prominent dorsal chaeta. Dental spine formula as 5–6/4, **2**;

all spines with evenly distributed numerous small denticles (Fig. 12E). Dens dorsally with ordinary chaetae and plumose chaetae, ventrally with dense scales. Mucronal outer basal tooth with toothlet, apical tooth subequal to subapical tooth, outer lamella with 5 intermediate teeth (Fig. 12F).

Differential diagnosis. *Tomocerus zayuensis* was described from Zayu County, Nyingchi, southeast Tibet on the basis of the long-preserved holotype. Our specimens from the same locality comply with the original description, including the colour pattern, the number of teeth on the claws and mucro, and the shape and formula of the dental spines. Compared to most other related species, in *T. zayuensis* the denticles on dental spines are much finer, and the distance between the two distal large spines is shorter. Besides, in this species the tenent hair guard chaetae are shorter than in most other related species, and the manubrial dorsal scales are numerous and arranged densely in strips, which is rather unusual among the *ocreatus* complex.

Habitat and distribution. In broadleaf litter in sample C9396, in mixed leaf litter in C9697 and C9396. The species is distributed in the southeast area of Tibet.

Material. Topotypes, 2 ♀ on slides, 'C9396 1–2 | *Tomocerus zayuensis*', (NJAU), CHINA, Tibet, Nyingchi, Zayu County, 2.viii.1997, Min Wu leg. — Other materials. 2 ♀ on slides, 'C9697 1–2 | *Tomocerus zayuensis*', (NJAU), CHINA, Tibet, Nyingchi, Lunang Town, N29°46′29.59″ E94°44′32.382″, 3326±14 m, 18.viii.2012, Feng Zhang leg.; 1 ♀ on slide, 'C9379 | *Tomocerus zayuensis*', 3 in alcohol, 'C9379', (NJAU), CHINA, Tibet, Lhoka, Qusum County, 4100 m, 26.vi.1997, Min Wu leg.

Tomocerus zhuque Yu sp.n.

Figs. 3H, 13; Table 1

Description. ***Size and colouration***: Body length 3.3–4.8 mm. General background colouration of body pale yellowish white to light yellow, head usually darker yellow. Ant. I and Ant. II distally with diffuse purple pigment, Ant III gradually darker towards apex, Ant. IV dark purple. Antennal base dorsally and ventrally with purple pigment. Eye patches black. Purple pigment diffusely around mouthparts. Tibiotarsi with diffuse purple pigment. Larger specimens (> 4.5 mm) darker yellow, with additional diffuse purple pigment on legs, especially on hind femur (Fig. 3H). ***Head***: Antenna 0.8–0.9× length of body. Length ratio of Ant I : II : III : IV = 1.0 : 1.3–1.5 : 8.1–9.0 : 1.3–1.4. Ant. III basally scaled. PAO absent. Eyes 6+6. Dorsal and ventral sides of head scaled. Cephalic dorsal macrochaetotaxy: anterior area: 2, 4; interocular area: 2, 7, central unpaired macrochaeta present; postocular area: 2+2; posterior area: 3+3. Posterior margin of head with approximately 30+30 small chaetae (Fig. 13A). ***Body chaetotaxy*** (Fig. 13B): Th. II with file of macrochaetae behind anterior margin. Number of macrochaetae or large mesochaetae in posterior row as 3, 3/ 3, 3, 4, 2, 4 from Th. II to Abd. V. Th. II with six central macrochaetae, inner five arranged approximately in triangular pattern, postero-central macrochaeta near pseudopore; Th. III with anterior macrochaeta; Abd. III with two anterior macrochaetae; Abd. IV with one antero-lateral macrochaeta; Abd. VI with numerous chaetae of different sizes. ***Legs***: Front, middle and hind tibiotarsi ventrally with 5–6, 6–7, 7–8 spine-like chaetae. Tenent hair clavate on all legs, subequal to inner edge of unguis in length; accessory chaetae small, weaker than pretarsal chaetae; guard chaetae 0.8–0.9× length of tenent hair. Unguis slender, with baso-internal ridges about 1/3 distance from base; lateral teeth pointed, of moderate size. Inner edge of unguis with small basal tooth and 4–5 more distal teeth, sub-basal tooth stronger than others. Unguiculus lanceolate, 0.5–0.7× length of unguis, its inner edge with 1 small tooth (Fig. 13C). ***Abdominal appendages***: Ventral tube scaled on both faces, anterior face with 40–55 chaetae on each side, posterior face with about 85–100 chaetae, each lateral flap with 80–140 chaetae and without scales. Anterior face of tenaculum with 11–17 chaetae, without scales (Fig. 13D). Ratio manubrium : dens : mucro = 3.3–3.7 : 4.2–4.6 : 1.0. Manubrium ventrally scaled without chaetae; laterally with large round scales and 9–11 chaetae, proximal chaeta small, distal chaetae strong; each dorsal chaetal strip with 190–240 chaetae of different sizes, blunt prominent chaeta at about 2/3–3/4 length from base of manubrium, 1–2 irregular rows of scales along inner edge and 9–14 pseudopores on lateral side (Fig. 13E); external corner chaeta as large as moderate-size mesochaetae in chaetal strip. Dens basally with blunt prominent dorsal chaeta. Dental spine formula as 1–2, **3**–**4**/4–5, **2**, proximal spines arranged in two rows, larger spines in outer row; all spines with evenly distributed numerous small denticles (Fig. 13F). Dens dorsally with ordinary chaetae and plumose chaetae, ventrally with dense scales. Mucronal outer basal tooth with toothlet, apical tooth slightly stronger than subapical tooth, outer lamella with 5–7 intermediate teeth (Fig. 13G).

Differential diagnosis. *Tomocerus zhuque* sp.n. is similar to *T. zayuensis* and *T. huangi* sp.n. in the chaetotaxy and fine structure of dental spines, but is mainly different from the latter in the presence of blunt manubrial prominent chaetae and arrangement of proximal dental spines in two rows. Besides, in *T. zhuque* sp.n. there are more chaetae on tenaculum than in *T. huangi* sp.n., and the subbasal ungual tooth is weaker than in the latter species.

Habitat and distribution. In mixed leaf litter. The species is so far known only from Zhuque National Forest Park, northern slope of eastern Qinling Cordillera.

Etymology. Named after the Chinese mythical bird Zhuque, the symbol god of the fire element and the direction south, and also the name of the national forest park where the species was collected.

Material. Holotype ♀ on slide, 'C9682 1 | *Tomocerus zhuque* | holotype', (NJAU), CHINA, Shaanxi Province, Xi'an, Hu County, Zhuque National Forest Park, N33°47′11.967″ E108°34′33.885″, 1599 m, 11.vii.2012, Feng Zhang, Yuanhao Ren, Zhen Chen & Xin Sun leg. — Paratypes, 4 ♀ on slides, 'C9682 2–3 | *Tomocerus zhuque* | paratype' and 'C9685 4–5 | *Tomocerus zhuque* | paratype',

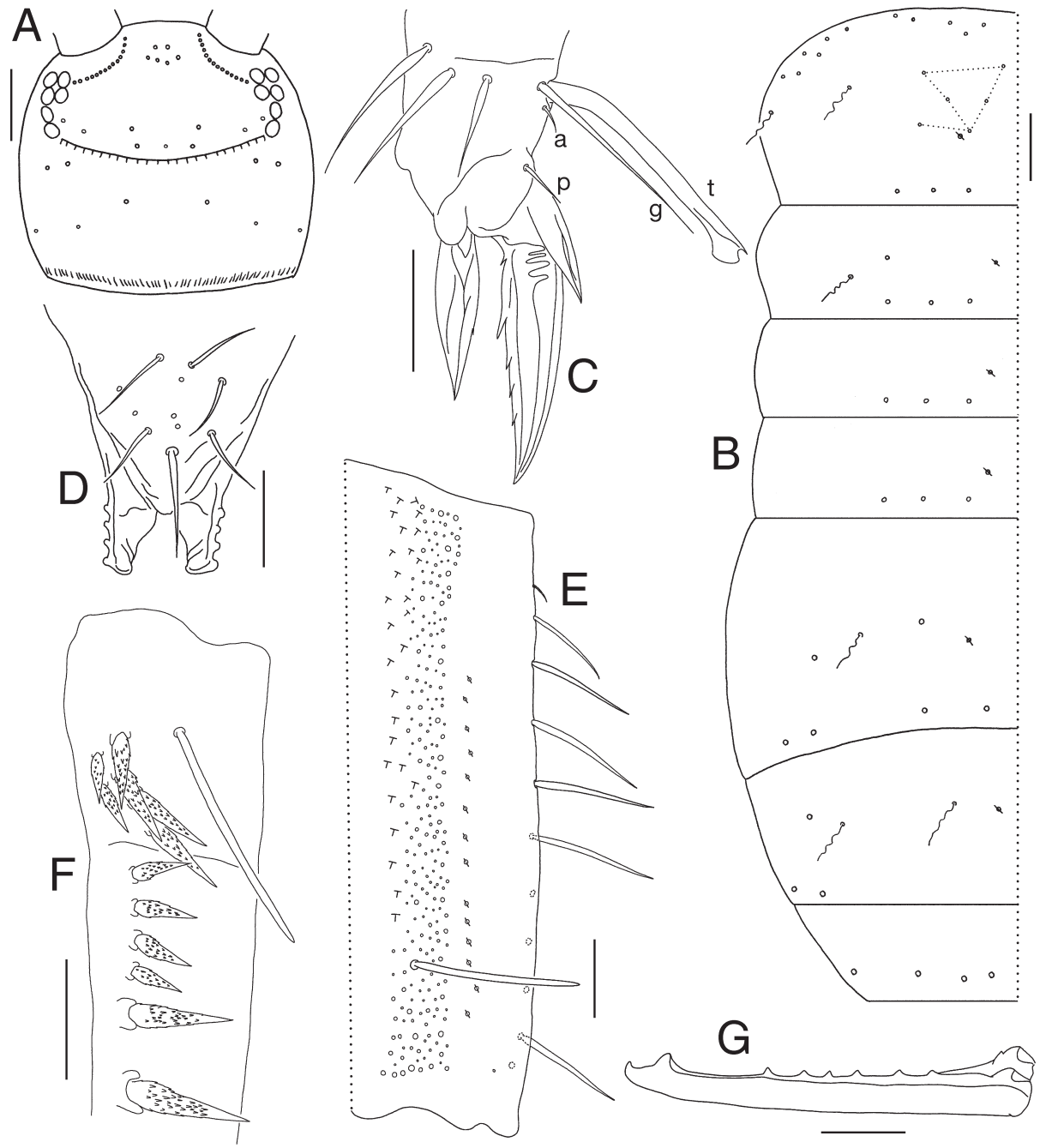

Fig. 13. *Tomocerus zhuque* sp.n. **A**: Cephalic dorsal chaetotaxy, dorsal view. **B**: Dorsal chaetotaxy of Th. II–Abd. V, dorsal view. **C**: Hind claw, lateral view. **D**: Tenaculum, anterior view. **E**: Right side of manubrium, dorsal view. **F**: Dental spines, dorsal view. **G**: Mucro, inner view. (Scale bars: A, B = 200 μm; C, D, G = 50 μm; E, F = 100 μm)

4 in alcohol, 'C9682' and 'C9685', (NJAU), same area as holotype, N33°47′11.967″–33°48′47.72″ E108°34′33.885″–108°35′47.23″, 1599–1933 m.

Key to species of *Tomocerus ocreatus* complex

1 PAO large, its long axis at least as long as diameter of cornea. Cave-dwelling species **2**
1' PAO not distinct or absent. Surface-dwelling species **5**
2 Anterior area of head with 2 macrochaetae **3**
2' Anterior area of head with 2, 2 macrochaetae **4**
3 Labral formula 4/5, 5, 4; interocular area of head without macrochaetae; vesicles of ventral tube with 6–8 tentacle-like papillae on either side ..... ***T. cthulhu* Yu & Li**
3' Labral formula 6/5, 5, 4; interocular area of head with 2 macrochaetae; vesicles of ventral tube normal ..... ***T. deharvengi* Yu & Li**
4 Labral formula 4/5, 5, 4; interocular area of head with 2, 3 macrochaetae ..... ***T. dong* Yu & Li**
4' Labral formula 6/5, 5, 4; interocular area of head with 2 macrochaetae ..... ***T. postantennalis* Yu & Li**

5 Thoracic terga with distinct lateral pigment bands (Fig. 2, Fig. 3E,F) **6**
5' Lateral sides of thoracic terga pale or with only diffuse pigment (Fig. 3A,B,C,D,G,H) **13**
6 Dens with small spine(s) between 2 distal large spines **7**
6' Dens without small spine(s) between 2 distal large spines **9**
7 Abd. III and Abd. IV dorsally with 1 and 2 dark purple patches on each side, respectively ..... ***T. hexipunctatus* Sun, Liang & Huang**
7' Abd. III/IV dorsally without dark purple patches ... **8**
8 Ant. I and II deep purple, lateral sides of abdominal segments without dark bands ..... ***T. baibungensis* Sun, Liang & Huang**
8' Ant. I and II not deep purple, lateral sides of abdominal segments with wide dark bands ..... ***T. folsomi* Denis**
9 Unguis with 1 middle tooth ..... ***T. wushanensis* Sun, Liang & Huang**
9' Unguis with more than 4 teeth **10**
10 Each side of manubrium and dens with 1 blunt prominent chaeta, respectively; dental spines with small denticles ..... ***T. qixiaensis* Yu**
10' Manubrium and dens without blunt prominent chaeta; dental spines with moderate to large denticles **11**
11 Inner sides of femora and basal parts of tibiotarsi with dark purple bands; interocular area of head without central macrochaeta, Th. II with 1 central macrochaeta ..... ***T. virgatus* sp.n.**
11' Legs without pigment bands; interocular area of head with central macrochaeta, Th. II with 5 or more central macrochaetae **12**
12 Manubrium with dorsal scales; thoracic terga with lateral broad pigment bands (Fig. 2) .... ***T. qinae* Yu**
12' Manubrium without dorsal scales; thoracic terga with lateral narrow pigment bands (Fig. 3F) ..... ***T. yueluensis* sp.n.**
13 Anterior area of head with 2, 2 macrochaetae **14**
13' Anterior area of head with 2, 4 macrochaetae **15**
14 Body colour pale white, head slightly grey; antenna as long as body; dental spines with moderate-size denticles ..... ***T. ocreatus* Denis**
14' Body colour grey; antenna half length of body; dental spines with small denticles ..... ***T. jiuzhaiensis* Liu, Zhou & Zhang**
15 Dens with 1 distal large spine ..... ***T. spinulus* Chen & Christiansen**
15' Dens with 2 distal large spines **16**
16 Manubrium without blunt prominent chaetae **17**
16' Manubrium with blunt prominent chaetae **18**
17 Sub-basal tooth on unguis distinctly stronger than other teeth (Fig. 5C); tenaculum with 2–5 chaetae; manubrium with 1 rough row of dorsal scales on each side (Fig. 5D) ..... ***T. huangi* sp.n.**
17' Sub-basal tooth on unguis only slightly larger than other teeth (Fig. 12C); tenaculum with about 15 chaetae; manubrium with 3–4 rough rows of dorsal scales on each side (Fig. 12D) ..... ***T. zayuensis* Huang & Yin**
18 Dens basally with blunt prominent chaeta; denticles evenly distributed on dental spine **19**
18' Dens basally without blunt prominent chaeta; denticles unevenly distributed on dental spine, with moderate to large denticles around base **20**
19 Manubrium with 2+2 blunt prominent chaetae; basal dental spines arranged in 1 row; spines with moderate-size denticles ..... ***T. pseudocreatus* sp.n.**
19' Manubrium with 1+1 blunt prominent chaetae; basal dental spines arranged in 2 rows; spines with small denticles ..... ***T. zhuque* sp.n.**
20 Furca ratio 8 : 9 : 1; distal part of dental spine serrated, with numerous tiny denticles; mucro with 8–11 intermediate teeth ..... ***T. deogyuensis* Lee**
20' Furca ratio 3.8–4.2 : 5.1–5.8 : 1.0; distal part of dental spine smooth, with fine longitudinal ribs; mucro with 4–7 intermediate teeth ..... ***T. changbaishanensis* Wang**

4. Discussion

4.1. Species delimitation by integrative approaches

Molecular delimitation has been successful in discriminating morphologically similar species of Collembola in several studies (Soto-Adames 2002; Felderhoff et al. 2010; Porco et al. 2010; Schneider & D'Haese 2013; Porco et al. 2014; Katz et al. 2015; Pan et al. 2015; Barjadze et al. 2016). The extensive cryptic diversity of the Chinese *ocreatus* complex was previously reported by Zhang et al. (2014), which also revealed that COI and 16S performed better than 28S D1–2 in species delimitation, and the single-locus method using a general mixed Yule coalescent (GMYC) model (Pons et al. 2006; Monaghan et al. 2009; Fujisawa & Barraclough 2013) estimated more MOTUs than the Bayesian multi-locus method (BP&P, Yang & Rannala 2010). In the present study, we employed the ABGD method and Bayesian PTP approaches on an updated data set of COI sequences and yielded similar results as Zhang et al. (2014) in recovering diversity. However, discordance still existed across results from different analyses, which could probably be attributed to the limitations of each method (Carstens et al. 2013), and to incomplete sampling of populations (Lohse 2009; Papadopoulou et al. 2009; Chesters et al. 2013), given the usually low density of tomocerids in most sampling areas. These limitations can be compensated for, but are not likely to be eliminated only by complementary molecular markers or approaches (Puillandre et al. 2012; Carstens et al. 2013). Compared to Zhang et al. (2014), who focused mainly on genetic diversity, the present study also included morphological examination. As expected, the morphological

characters had lower resolution than the molecular approaches. Only three AGs were successfully recognized with traditional characters, while the newly emphasized characters provided reliable diagnosis of six more AGs, leaving the other 11 AGs in four MGs (Table 1). In addition to the examined characters, when colouration, such as the darkness and coverage of bluish-purple pigment on terga and appendages, were considered, different colour forms could be recognized among the morphologically unsolved AGs (Fig. S2). It is expected that more undescribed species exist among those colour forms. Nevertheless, more material is required to assess the inter- and intraspecific variability before using colouration alone as critical morphological diagnosis for *Tomocerus* species.

4.2. Evaluation of taxonomic characters previously omitted or underestimated

In the present study, detailed morphological examination together with molecular evidences has improved our understanding towards some taxonomic characters for the genus *Tomocerus*, and potentially for the whole subfamily.

Tergal chaetotaxy is a significant taxonomic character for Collembola, but in Tomoceridae it was considered rather constant (Yosii 1967), until Felderhoff et al. (2010), Yu et al. (2014) and Barjadze et al. (2016) demonstrated the importance of the details of macrochaetotaxy in *Pogonognathellus*, *Monodontocerus* Yosii, 1955 and *Plutomurus*, respectively. In the *ocreatus* complex the dorsal chaetotaxy on Th. II is variable across species as shown in our descriptions. Even though the number of macrochaetae is the same, their position and arrangement are important. For example, in *T. virgatus* sp.n. and *Tomocerus cthulhu* Yu & Li, 2016, the distance between the single central macrochaeta and the pseudopore is different, indicating this chaeta may be heterologous in postembryonic development in different species. In the *ocreatus* complex, a typical complete pattern of chaetotaxy can be drawn in the central area of Th. II, that five macrochaetae arranged roughly in a triangle, with another macrochaeta lateral to them (Figs. 4B, 5B, 7B, 12B, 13B); in some species, a number of chaetae are missing from this pattern (Figs. 6B, 9B, 10B). This chaetotaxical pattern is easily recognized and sufficient for the identification of most species. However, to avoid misidentification of certain chaetae in subsequent phylogenetic studies, a nomenclatural system is required. Such systems have been proposed by Szeptycki (1972) and Yu et al. (2016c) for the first instars of *Pogonognathellus* and *Tomocerina*, and by Barjadze et al. (2016) for the adult of *Plutomurus*. The systems for first instar were based on the homology of chaetae, but sharp differences between primary and developed chaetotaxy makes it difficult to use for adults; the system for adult *Plutomurus* was directly introduced from that for Entomobryidae (Jordana & Baquero 2005; Greenslade & Jordana 2014), which has a pattern of chaetotaxy distinct from that of Tomoceridae (Szeptycki 1979; Yu et al. 2016c). Hence a more reliable nomenclatural system for the adult should be established in future study on the basis of homology after observing postembryonic development in various groups of Tomoceridae.

The manubrium of furca bears several taxonomic characters, including dorsal chaetae and dorsal scales. The prominent dorsal chaetae were emphasized in *Pogonognathellus* by Maynard (1951). Yosii (1967) recorded these chaetae in other species, and noticed that the shape of these chaetae could be either blunt or pointed. But this character was often insufficiently described or omitted. In the present study, several observed species have distinct prominent chaetae with variable numbers and position. These prominent chaetae can be used to differentiate between some species, such as *T. yueluensis* sp.n. and *T. pseudocreatus* sp.n. However, they are easily damaged or lost during specimen collection and slide preparation, thus should be treated cautiously. Besides the prominent chaetae, Yosii (1967) also noticed that the manubrial dorsal scales were a possible character with species delimiting utility. In the *ocreatus* complex, these scales can be either present or absent. If present, the scales are usually in 1–2 very narrow rows along the inner side of chaetal strips, but in *T. zayuensis*, the dorsal scales are densely arranged in broad strips, indicating the number and arrangement of these scales are also valuable in taxonomy.

The shape of the dental spines is an important diagnostic character for tomocerid taxa. Traditional descriptions generally summarize the shape of spines into several types, such as simple, compound, bifurcate or trifurcate, but seldom distinguish further details. Our study showed an interspecific gradient in the size, number and distribution of denticles on the compound-type spines. For example, *T. ocreatus* has almost evenly distributed moderate-size denticles (Denis 1948; Yu et al. 2016a), *T. huangi* sp.n. has more densely distributed finer denticles, and *T. changbaishanensis* has basally distributed moderate to large denticles. Similarly, the fine sculpture of the simple-type spines can also be variable in different groups (Zhang et al. 2014). As far as we observed, the superficial sculpture of dental spines has more interspecific difference than intraspecific variation, therefore, this character is valuable in taxonomy, and we suggest that future descriptions should provide more details on the fine structure of dental spines.

4.3. Species diversity of the *Tomocerus ocreatus* complex

The Chinese *ocreatus* complex was proved to be a monophyletic group within the genus (Zhang et al. 2014). Both Zhang et al. (2014) and the present study detected high diversity within the complex. In the former study, all morphologically undefined MOTUs were considered as

the result of cryptic diversity within a complex, while the present study has detected considerable morphological variances among the MOTUs and described five species new to science according to a set of species validation criteria. Compared to the previously considered wide distribution of *T. ocreatus*, most detected taxa within the *ocreatus* complex are regional or endemic; in some localities two or more different forms were found together, for example AG1/9/13, AG5/17 and AG17/18, suggesting the existence of more species/groups in a wider range of areas that have not been sampled.

As supported by previous records, Tomoceridae should be less diversified in the oriental realm (south) than in the palaearctic realm (north) (Yu et al. 2016a). However, most *ocreatus*-type species are present to the south of the Qinling-Dabie Mountains, indicating the family is also highly diversified in the oriental realm. As we have observed, tomocerids often account for a larger proportion of the epigeic and epedaphic Collembola abundance in the boreal forest, while in the southern areas entomobryids and paronellids are normally dominant, and tomocerids are usually in low abundance and are likely to be omitted if not searched specially during sampling, hence the diversity could be easily underestimated.

Besides the species involved in this study, other species such as *T. baibungensis* Sun, Liang & Huang, 2006, *T. wushanensis* Sun, Liang & Huang, 2007, *T. hexipunctatus* Sun, Liang & Huang 2007 and *T. jiuzhaiensis* Liu, Zhou & Zhang, 2013 morphologically comply with the *ocreatus* complex. Yu et al. (2016a) made morphological review of the previous non-type records of *T. ocreatus* from different areas of Asia, and inferred that these records might be independent species within the *ocreatus* complex. Further phylogeographic analyses including these species could increase our knowledge on the diversity and distribution of the *ocreatus*-type tomocerids, and further shed light on the historical dispersal and adaptive radiation of Tomoceridae in East Asia.

5. Acknowledgements

We thank Jianxiu Chen and Min Wu in Nanjing University, Zhixiang Pan in Taizhou University, Zhaohui Li and Yuanhao Ren in Nanjing Xiaozhuang University for their assistance in collecting the specimens. This work was supported by the National Natural Science Foundation of China (41501056 and 41371263), the Fundamental Research Funds for the Central Universities (KYZ201617 and KYTZ201404).

6. References

Barjadze S., Baquero E., Soto-Adames F.N., Giordano R., Jordana R. 2016. New diagnosis for species of *Plutomurus* Yosii (Collembola, Tomoceridae), with descriptions of two new species from Georgian caves. – Zootaxa **4126**: 77–96.

Börner C. 1908. Collembolen aus Südafrika, nebst einer Studie über die I. Maxille der Collembolen. In: Schultze L., Forschungsreise im westlichen und zentralen Südafrika. – Denkschriften der Medicinisch-naturwissenschaftlichen Gesellschaft zu Jena **13**: 53–68.

Carstens B.C., Pelletier T.A., Reid N.M., Satler J.D. 2013. How to fail at species delimitation. – Molecular Ecology **22**: 4369–4383.

Chen J.X., Ma Y.T. 1997. A new species of the genus *Tomocerus* (*s. s.*) (Collembola: Tomoceridae) from China. – Entomotaxonomia **19**: 157–160.

Chesters D., Yu F., Cao H.X., Dai Q.Y., Wu Q.T., Shi W., Zheng W., Zhu C.D. 2013. Heuristic optimization for global species clustering of DNA sequence data from multiple loci. – Methods in Ecology and Evolution **4**: 961–970.

Chiba S. 1968. Collembola of the Mt. Hakkoda area. I. Family Tomoceridae. – The Science Reports of the Hirosaki University **15**: 24–26.

Christiansen K. 1964. A revision of the Nearctic members of the genus *Tomocerus* (Collembola: Entomobryidae). – Revue d'Ecologie et de Biologie du Sol **1**: 668–675.

Darriba D., Taboada G.L., Doallo R., Posada D. 2012. jModelTest 2: more models, new heuristics and parallel computing. – Nature Methods **9**: 772.

Deharveng L. 2004. Recent advances in Collembola systematics. – Pedobiologia **48**: 415–433.

Denis J.R. 1929. Notes sur les collemboles récoltés dans ses voyages par le Prof. F. Silvestri. – Bollettino del Laboratorio di Zoologia Generale e Agraria della R. Scuola Superiore d'Agricoltura in Portici **22**: 166–180.

Denis J.R. 1948. Collemboles d'Indochine. – Notes d'Entomologie Chinoise **12**: 183–311.

Felderhoff K.L., Bernard E.C., Moulton J.K. 2010. Survey of *Pogonognathellus* Börner (Collembola: Tomoceridae) in the Southern Appalachians based on morphological and molecular data. – Annals of the Entomological Society of America **103**: 472–491.

Fjellberg A. 2007. The Collembola of Fennoscandia and Denmark. Part II: Entomobryomorpha and Symphypleona. – Fauna Entomologica Scandinavica **42**: 1–264.

Folmer O., Black M., Hoeh W., Lutz R., Vrijenhoek R. 1994. DNA primers for amplification of mitochondrial cytochrome c oxidase subunit I from diverse metazoan invertebrates. – Molecular Marine Biology and Biotechnology **3**: 294–299.

Folsom J.W. 1913. North American spring-tails of the sub-family Tomocerinae. – Proceedings of the United States National Museum **46**: 451–472.

Forey E., Coulibaly S.F.M., Chauvat M. 2015. Flowering phenology of a herbaceous species (*Poa annua*) is regulated by soil Collembola. – Soil Biology and Biochemistry **90**: 30–33.

Fujisawa T., Barraclough T.G. 2013. Delimiting species using single-locus data and the generalized mixed Yule coalescent approach: a revised method and evaluation on simulated data sets. – Systematic Biology **62**: 707–724.

Greenslade P., Jordana R. 2014. Description and conservation status of a new species of *Australotomurus* (Collembola: Entomobryidae: Orchesellinae) from urban Perth remnant bushland. – Zootaxa **3872**: 561–576.

Hopkin S.P. 1997. Biology of the Springtails (Insecta: Collembola). – Oxford University Press, Oxford, New York. 330 pp.

Hoskins J.L., Janion-Scheepers C., Chown S.L., Duffy G.A. 2015. Growth and reproduction of laboratory-reared neanurid Collembola using a novel slime mould diet. – Scientific Reports **5**: 11957.

Jordana R., Baquero E. 2005. A proposal of characters for taxonomic identification of *Entomobrya* species (Collembola, Entomobryomorpha), with description of a new species. – Abhandlungen und Berichte des Naturkundemuseums Görlitz **76**: 117–134.

Katoh K., Standley D.M. 2013. MAFFT multiple sequence alignment software version 7: improvements in performance and usability. – Molecular Biology and Evolution **30**: 772–780.

Katz A.D., Giordano R., Soto-Adames F.N. 2015. Operational criteria for cryptic species delimitation when evidence is limited, as exemplified by North American *Entomobrya* (Collembola: Entomobryidae). – Zoological Journal of the Linnean Society **173**: 818–840.

Kimura M. 1980. A simple method for estimating evolutionary rates of base substitutions through comparative studies of nucleotide sequences. – Journal of Molecular Evolution **16**: 111–120.

Knowles L.L., Carstens B.C. 2007. Delimiting species without monophyletic gene trees. – Systematic Biology **56**: 887–895.

Kopecky O., Novak K., Vojar J., Susta F. 2016. Food composition of alpine newt (*Ichthyosaura alpestris*) in the post-hibernation terrestrial life stage. – North-Western Journal of Zoology **12**: 299–303.

Lee B.H. 1975. Étude de la faune coréenne des Insectes Collemboles VI. Sur la famille des Tomoceridae, édaphiques, avec la description de quatre nouvelles espèces et d'une nouvelle sous-espèce. – Bulletin du Muséum National d'Histoire Naturelle **317**: 945–961.

Liu Y.Q., Zhou J.H., Zhang Q.D. 2013. A new species of the genus *Tomocerus* (Collembola, Tomoceridae) from China. – Acta Zootaxonomica Sinica **38**: 289–292.

Lohse K. 2009. Can mtDNA barcodes be used to delimit species? A response to Pons et al. (2006). – Systematic Biology **58**: 439–442.

Lubbock J. 1862. Notes on the Thysanura. Part II. – The Transactions of the Linnean Society of London **23**: 589–601.

Ma Y.T. 2004. Taxonomic study on the genera *Dicranocentrus* and *Entomobrya* and the family Tomoceridae from China (Insecta: Apterygota). – PhD thesis, Nanjing University, Nanjing, China.

Martynova E.F. 1977. Springtails of the family Tomoceridae (Collembola) from the fauna of the Far East. – Insect Fauna of the Far East **46**: 3–16.

Maynard E.A. 1951. A monograph of the Collembola or springtail insects of New York State. – Comstock Publishing Company, Ithaca, New York. 339 pp.

Miller M.A., Pfeiffer W., Schwartz T. 2010. Creating the CIPRES Science Gateway for inference of large phylogenetic trees. Pp. 1–8 in: Proceedings of the Gateway Computing Environments Workshop (New Orleans, November 14, 2010).

Monaghan M.T., Wild R., Elliot M., Fujisawa T., Balke M., Inward D.J.G., Lees D.C., Ranaivosolo R., Eggleton P., Barraclough T.G., Vogler A.P. 2009. Accelerated species inventory on Madagascar using coalescent-based models of species delineation. – Systematic Biology **58**: 298–311.

Nyffeler M., Birkhofer K. 2017. An estimated 400–800 million tons of prey are annually killed by the global spider community. – Die Naturwissenschaften **104**: 30.

O'Meara B.C. 2010. New heuristic methods for joint species delimitation and species tree inference. – Systematic Biology **59**: 59–73.

Pan Z.X., Zhang F., Li Y.B. 2015. Two closely related *Homidia* species (Entomobryidae, Collembola) revealed by morphological and molecular evidence. – Zootaxa **3918**: 285–294.

Papadopoulou A., Monaghan M.T., Barraclough T.G., Vogler A.P. 2009. Sampling error does not invalidate the Yule-coalescent model for species delimitation. A response to Lohse (2009). – Systematic Biology **58**: 442–444.

Park K.H., Bernard E.C., Moulton J.K. 2011. Three new species of *Pogonognathellus* (Collembola: Tomoceridae) from North America. – Zootaxa **3070**: 1–14.

Pons J., Barraclough T.G., Gomez-Zurita J., Cardoso A., Duran D.P., Hazell S., Kamoun S., Sumlin W.D., Vogler A.P. 2006. Sequence based species delimitation for the DNA taxonomy of undescribed insects. – Systematic Biology **55**: 595–609.

Porco D., Bedos A., Deharveng L. 2010. Description and DNA barcoding assessment of the new species *Deutonura gibbosa* (Collembola: Neanuridae: Neanurinae), a common springtail of Alps and Jura. – Zootaxa **2639**: 59–68.

Porco D., Bedos A., Greenslade P., Janion-Scheepers C., Skarżyński D., Stevens M.I., Jansen van Vuuren B., Deharveng L. 2012. Challenging species delimitation in Collembola: cryptic diversity among common springtails unveiled by DNA barcoding. – Invertebrate Systematics **26**: 470–477.

Porco D., Skarżyński D., Decaëns T., Hebert P.D.N., Deharveng L. 2014. Barcoding the Collembola of Churchill: a molecular taxonomic reassessment of species diversity in a sub-Arctic area. – Molecular Ecology Resources **14**: 249–261.

Potapov A.A., Semenina E.E., Korotkevich A.Yu., Kuznetsova N.A., Tiunov A.V. 2016. Connecting taxonomy and ecology: Trophic niches of collembolans as related to taxonomic identity and life forms. – Soil Biology and Biochemistry **101**: 20–31.

Puillandre N., Lambert A., Brouillet S., Achaz G. 2012. ABGD, Automatic Barcode Gap Discovery for primary species delimitation. – Molecular Ecology **21**: 1864–1877.

Rambaut A., Drummond A.J. 2007. Tracer v1.4. – Available at http://beast.bio.ed.ac.uk/Tracer/.

Reibe K., Götz K.P., Ross C.L., Döring T.F., Ellmer F., Ruess L. 2015. Impact of quality and quantity of biochar and hydrochar on soil Collembola and growth of spring wheat. – Soil Biology and Biochemistry **83**: 84–87.

Ronquist F., Teslenko M., van der Mark P., Ayres D.L., Darling A., Höhna S., Larget B., Liu L., Suchard M.A., Huelsenbeck J.P. 2012. MrBayes 3.2: Efficient Bayesian phylogenetic inference and model choice across a large model space. – Systematic Biology **61**: 539–542.

Salmon S., Ponge J.F., Gachet S., Deharveng L., Lefebvre N., Delabrosse F. 2014. Linking species, traits and habitat characteristics of Collembola at European scale. – Soil Biology and Biochemistry **75**: 73–85.

Schäffer C. 1896. Die Collembola der Umgebung von Hamburg und benachbarter Gebiete. – Jahrbuch der Hamburgischen Wissenschaftlichen Anstalten **13**: 150–216.

Schneider C., D'Haese C.A. 2013. Morphological and molecular insights on *Megalothorax*: the largest Neelipleona genus revisited (Collembola). – Invertebrate Systematics **27**: 317–364.

Soto-Adames F.N. 2002. Molecular phylogeny of the Puerto Rican *Lepidocyrtus* and *Pseudosinella* (Hexapoda: Collembola), a validation of Yoshii's 'color pattern species'. – Molecular Phylogenetics and Evolution **25**: 27–42.

Stamatakis A. 2014. RAxML Version 8: A tool for Phylogenetic Analysis and Post-Analysis of Large Phylogenies. – Bioinformatics **30**: 1312–1313.

Sun Y., Liang A.P., Huang F.S. 2006. Descriptions of two new Tibetan species of *Tomocerus* (*s. str.*) Nicolet, 1842 (Collembola, Tomoceridae). – Acta Zootaxonomica Sinica **31**: 559–563.

Sun Y., Liang A.P., Huang F.S. 2007. The genus *Tomocerus* Nicolet (Collembola: Tomoceridae) from Sichuan, China, with description of two new species. – Proceedings of the Entomological Society of Washington **109**: 572–578.

Sun Y., Liang A.P., Huang F.S. 2007. The genus *Tomocerus* Nicolet (Collembola, Tomoceridae) from Hunan, China with description of two new species. – Acta Zootaxonomica Sinica **32**: 52–55.

Sun X., Zhang F., Ding Y.H., Davies T.W., Li Y., Wu D.H. 2017. Delimiting species of *Protaphorura* (Collembola: Onychiuridae): integrative evidence based on morphology, DNA sequences and geography. – Scientific Reports **7**: 8261, 1–9.

Szeptycki A. 1972. Morpho-systematic studies on Collembola. III. Body chaetotaxy in the first instars of several genera of the Entomobryomorpha. – Acta Zoologica Cracoviensia **17**: 341–372.

Szeptycki A. 1979. Morpho-systematic studies on Collembola. IV. Chaetotaxy of the Entomobryidae and its phylogenetical significance. – Polska Akademia Nauk, Kraków. 218 pp.

Tamura K., Peterson D., Peterson N., Stecher G., Nei M., Kumar S. 2011. MEGA5: Molecular evolutionary genetics analysis using maximum likelihood, evolutionary distance, and maximum parsimony methods. – Molecular Biology and Evolution **28**: 2731–2739.

Widenfalk L.A., Malmström A., Berg M.P., Bengtsson J. 2016. Small-scale Collembola community composition in a pine forest soil-overdispersion in functional traits indicates the importance of species interactions. – Soil Biology and Biochemistry **103**: 52–62.

Yang Z., Rannala B. 2010. Bayesian species delimitation using multilocus sequence data. – Proceedings of the National Academy of Sciences of the United States of America **107**: 9264–9926.

Yin Z.W., Cai C.Y., Huang D.Y., Li L.Z. 2017. Specialized adaptations for springtail predation in Mesozoic beetles. – Scientific Reports **7**: 98.

Yosii R. 1955. Meeresinsekten der Tokara Inseln. 4. Collembolen nebst Beschreibungen terrestrischer Formen. – Publications of the Seto Marine Biological Laboratory **4**: 379–401.

Yosii R. 1956. Monographie zur Höhlencollembolen Japans. – Contributions from the Biological Laboratory Kyoto University **3**: 1–109.

Yosii R. 1967. Studies on the collembolan family Tomoceridae, with special reference to Japanese forms. – Contributions from the Biological Laboratory Kyoto University **20**: 1–54.

Yu D.Y., Deharveng L., Zhang F. 2014. New species of *Monodontocerus* (Collembola: Tomoceridae) from southern China with diagnostic notes on the genus and introduction of new taxonomic characters. – Zootaxa **3768**: 557–575.

Yu D.Y., Man L.C., Deharveng L. 2016a. Tomoceridae (Collembola, Entomobryomorpha) from the southern Annamitic cordillera: redescription of *Tomocerus ocreatus* Denis, 1948 and description of a new species of *Tomocerina* Yosii, 1955. – European Journal of Taxonomy **176**: 1–14.

Yu D.Y., Yao J., Hu F. 2016b. Two new species of *Tomocerus ocreatus* complex (Collembola, Tomoceridae) from Nanjing, China. – Zootaxa **4084**: 125–134.

Yu D.Y., Zhang F., Stevens M.I., Yan Q.B., Liu M.Q., Hu F. 2016c. New insight into the systematics of Tomoceridae (Hexapoda, Collembola) by integrating molecular and morphological evidence. – Zoologica Scripta **45**: 286–299.

Yu D.Y., Li Y.B. 2016. New troglomorphic species of *Tomocerus* with well-developed postantennal organs (Collembola: Tomoceridae). – Zootaxa **4162**: 361–372.

Zhang C., Rannala B., Yang Z. 2012. Robustness of compound Dirichlet priors for Bayesian inference of branch lengths. – Systematic Biology **61**: 779–784.

Zhang F., Yu D.Y., Luo Y.Z., Ho S.Y.W., Wang B.X., Zhu C.D. 2014. Cryptic diversity, diversification and vicariance in two species complexes of *Tomocerus* (Collembola, Tomoceridae) from China. – Zoologica Scripta **43**: 393–404.

Zhang J., Kapli P., Pavlidis P., Stamatakis A. 2013. A general species delimitation method with applications to phylogenetic placements. – Bioinformatics **29**: 2869–2876.

Zhu D., Ke X., Wu L.H., Christie P., Luo Y.M. 2016. Biological transfer of dietary cadmium in relation to nitrogen transfer and ^{15}N fractionation in a soil collembolan-predatory mite food chain. – Soil Biology and Biochemistry **101**: 207–216.

Electronic Supplement Files

at http://www.senckenberg.de/arthropod-systematics

File 1: yu&al-tomocerusocreatus-asp2018-electronicsupplement-1.xls — **Table S1.** Information of analyzed sequences: specimen code, identity, grouping, collection locality, GenBank accession number and source. Source: 1, this study; 2, Zhang et al. 2014; 3, Yu et al. 2016; 4, Yu et al. 2017. — **Table S2.** Pairwise genetic distances among haplotypes of mitochondrial COI sequences based on K2P substitution model, with maximum within group distance marked green and maximum/minimum between group distances marked red.

File 2: yu&al-tomocerusocreatus-asp2018-electronicsupplement-2.pdf — **Fig. S1.** Neighbour-joining tree based on mitochondrial COI sequences, showing bootstrap values and species grouping. — **Fig. S2.** Habitus of undefined groups (represented by AGs and MGs). (Scale bars: 1 mm).

Zoobank Registrations

at http://zoobank.org

Present article: http://zoobank.org/urn:lsid:zoobank.org:pub:0207DD6A-E88F-4CF4-B0EB-4E37625D0C20

***Tomocerus huangi* Yu, 2018:** http://zoobank.org/urn:lsid:zoobank.org:act:432509C0-F203-4EAB-986F-38B3353056C0

***Tomocerus pseudocreatus* Yu, 2018:** http://zoobank.org/urn:lsid:zoobank.org:act:1837D4A9-F959-408A-8F01-B7578F318169

***Tomocerus virgatus* Yu, 2018:** http://zoobank.org/urn:lsid:zoobank.org:act:EBE1623B-8D55-485A-8BFC-425A751D91EC

***Tomocerus yueluensis* Yu, 2018:** http://zoobank.org/urn:lsid:zoobank.org:act:E4AA70E6-FF30-422E-A39A-B1B6AA8A0B16

***Tomocerus zhuque* Yu, 2018:** http://zoobank.org/urn:lsid:zoobank.org:act:89D7E22D-C109-475E-8610-E1657B3A0AB5